Journal of Petroleum Science and Engineering 220 (2023) 111202

Contents lists available at ScienceDirect

Journal of Petroleum Science and Engineering

journal homepage: www.elsevier.com/locate/petrol

Field performance and numerical simulation study on the toe to heel air injection (THAI) process in a heavy oil reservoir with bottom water

Hossein Anbari [a,*], John P. Robinson [a], Malcolm Greaves [b], Sean P. Rigby [a,**]

[a] Faculty of Engineering, University of Nottingham, Nottingham, NG7 2RD, UK
[b] Department of Chemical Engineering, University of Bath, Bath, BA2 7AY, UK

ARTICLE INFO

Keywords:
Enhanced oil recovery
Heavy oil recovery
In-situ combustion
Toe-to-heel air injection
Reservoir engineering
Numerical modelling

ABSTRACT

Extra-heavy oil and bitumen (EHOB) comprise 30 percent of the remaining recoverable fossil fuel resources on Earth. This means EHOB could play an important role in a secure transition towards net zero emissions (NZE) by 2050. Technological developments, such as toe to heel air injection (THAI), have been shown to efficiently recover heavy oil with reduced environmental footprint. The Kerrobert project was the first to utilise the THAI technology in presence of bottom water (BW) in the reservoir. The project demonstrated a good performance (with average oil rate of 10 m^3/day per well) compared to the conventional ISC operations in a BW situation. Lessons taken from the Kerrobert operational experience can assist the forthcoming THAI operations explicitly in the presence of BW. Dynamic field data for one of the best performing THAI pilot well pairs (K2), were analysed in this work. It was found that the K2 pilot must have experienced interference from K5, which is the closest neighbouring THAI well pair to the K2. Previously developed THAI models have not been validated against actual field data. A new field-scale THAI model in the presence of BW was constructed and, for the first time, validated against the field data from the Kerrobert project in this work. In addition, the quasi-staggered line drive well arrangement, as used for the K2 pilot, was studied. The daily and cumulative oil production rates were predicted well (the final agreement with field data was within 3 percent). The history matched model was then used to investigate the effect of the variation in air injection rates on THAI performance in presence of BW. Major developed zones during the propagation of the combustion front were numerically examined. It was demonstrated that extra air ingress from the neighbouring THAI well pair has caused a reduction in oxygen utilisation throughout the process. As a result, the simulated temperature profile declined with the increasing combustion time. The oxygen profile around the horizontal producer (HP) well was studied via the new history-matched model. An inversely proportional relationship was detected between the coke concentration and the oxygen profile around the HP well. It was found that the size of the steam zone, ahead of the combustion front, differs with variation in air injection rates. It was observed that some of the mobilised oil sank into the BW, leaving a significant amount of oil trapped in the reservoir. To prevent such an event, the location of the HP well was altered as a potential strategy to optimise the THAI efficiency. Consequently, the oxygen utilisation was improved by 13%, resulting in 73% higher cumulative oil production in comparison with the history-matched model.

1. Introduction

As the world makes its way towards net zero emissions, there is an ever-present risk of mismatch between energy supply and demand. If there are no further changes in current energy policies, oil demand in 2050 will remain above 100 million barrels per day (mb/day). By contrast, if governments pursue a 1.5 °C world temperature change stabilisation objective, then oil demand could drop to 24 mb/day by the same year. Extra-heavy oil and bitumen (EHOB) comprises 30 percent (only 4% less than conventional crude oil) of remaining technically recoverable fossil fuel resources on the earth (International Energy Agency, 2021). The attention has been shifting towards unconventional oil such as EHOB with the decline in conventional light oil reserves (Adam et al., 2020). However, EHOB are difficult to recover due to high

* Corresponding author.
** Corresponding author.
E-mail addresses: hossein.anbari@nottingham.ac.uk (H. Anbari), sean.rigby@nottingham.ac.uk (S.P. Rigby).

https://doi.org/10.1016/j.petrol.2022.111202
Received 3 May 2022; Received in revised form 20 September 2022; Accepted 30 October 2022
Available online 4 November 2022
0920-4105/© 2022 The Authors. Published by Elsevier B.V. This is an open access article under the CC BY license (http://creativecommons.org/licenses/by/4.0/).

intrinsic viscosity. Thermal enhanced oil recovery (EOR) methods are designed to reduce the viscosity of the remaining oil in place by increasing its temperature, requiring the injection of steam or air (in-situ combustion) (Greaves and Al-Shamali, 1996). Shah et al. (2010) reviewed novel thermal techniques for heavy oil recovery and bitumen extraction/upgrading. The methods that employ steam are steam flooding, cyclic steam stimulation (CSS), and steam assisted gravity drainage (SAGD). The main limitation for steam-based methods, is that they are very energy intensive as they use natural gas to provide required energy. Also, surface steam generation processes cause creation of significant quantities of greenhouse gases. Donnelly and Pendergast (1999) reported an average of around 0.10 tonnes of CO_2 equivalent per barrel of oil recovered by SAGD process, mainly to supply the latent heat requirement of steam generation. Additionally, large volumes of water are needed to run SAGD with between 2 and 10 barrels of water injected as steam for every barrel of oil produced (Shah et al., 2010).

In-situ combustion (ISC) involves injection of air into the reservoir and creation of a combustion front, in which a fraction of the oil in the reservoir is combusted to generate heat downhole. The high-volume combustion gases (produced from low volume oil) push fluids (including gas from injected air, e.g., nitrogen, and by-products of combustion, e.g., mobilised oil) ahead of the combustion zone. In the original concept of ISC, which uses a vertical injector well-vertical producer well arrangement, the combustion zone moves from the injector well towards the producer well over time. The conventional ISC process suffers from serious operational problems, with gas over-riding and channelling being especially problematic (Nasr and Ayodele, 2005; Xia and Greaves, 2006). Toe to Heel Air Injection (THAI) technology integrates in-situ combustion and advanced horizontal well concepts. A horizontal producer well is used instead of a vertical producer well (as in conventional ISC), and this difference is the main feature of the THAI process. Also, the toe of the horizontal producer is positioned close to the injection point. Thus, as the combustion front propagates along the horizontal production well, from the 'toe' position to the 'heel', only short, gravity-driven vertical displacement of oil is necessary compared to the longer, horizontal displacement needed for conventional ISC (Xia and Greaves, 2000). Controlled gas over-ride, high sweep efficiency, production of thermally upgraded heavy oil, and less environmental footprint have been reported as potential benefits of the THAI process (Xia and Greaves, 2006). Other beneficial attributes of the THAI process can be found in a study by Greaves et al. (2001), including its environmental benefits through recycling CO_2, reduction in energy requirement, and eliminating the water requirement compared to steam injection based heavy oil recovery technologies (e.g., SAGD). The water produced within the SAGD process must be cleaned up at the water treatment facilities at the surface. This is another loss associated with SAGD which can be eliminated by employing the THAI process. The THAI process can reduce the surface facility requirement leading to a dramatic reduction in capital and operational costs of heavy oil production, while diminishing emission intensity.

There have been seven THAI pilots/projects, located in 3 countries, since 2006 (Turta, 2021). Canada was the pioneer in field testing of THAI. The Whitesands Experimental THAI project (2006–2011), located in Conklin, Alberta province, was the first field pilot of the THAI process. The main objective for the Whitesands project was to evaluate the THAI process under actual reservoir conditions, in order to advance the technology sufficiently to undertake a commercial project (Ayasse et al., 2005). Based on the lessons taken from the Whitesands project, the Kerrobert project, located in Saskatchewan province, Canada, commenced in 2009 (and is still ongoing after 13 years). The Kerrobert THAI project is the first THAI pilot in a conventional heavy oil reservoir underlain by a relatively thick bottom water zone. The effect of bottom water on THAI performance was tested in the piloting stage of the Kerrobert project. So far, from both Canadian THAI projects, over half a million barrels of partially upgraded oil has been produced. However, the oil rate per well (10–30 m^3/day) was lower than in the SAGD projects (Turta et al., 2021). China (with 3 THAI projects since 2012) and India (with 2 THAI projects since 2016) are other countries that have also been utilising THAI technology for heavy oil recovery (Turta, 2021).

Numerical simulations are a key tool to investigate the THAI operating mechanism. Previously developed field-scale THAI models (Coates and Zhao, 2001; Greaves et al., 2012 a; Greaves et al., 2013; Ado, 2020) used data from 3D combustion cell experiments to first validate their laboratory scale THAI simulation and only then scale-up experimental scale models to field-scale models. However, none of the aforementioned models consider a bottom water zone. Although, Araujo et al. (2016), Ado (2019), and Ado et al. (2022) carried out THAI simulations in the presence of bottom water in the reservoir, their results were not validated against actual field data. Ado et al. (2022) found that the oil recovery is affected by how large the thickness of the bottom water layer is, and the severity of such was determined to be proportional to the thickness of the bottom water layer. Ado (2019) reported that the critical BW thickness, when the THAI process is implemented in a staggered line drive pattern, should lie in the range of 50% OL (oil layer thickness) $<$ BW $<$ 100 OL. *Ab initio* field-scale model development using direct history matching of a field-scale THAI process has never been tried previously by other workers. This was due to insufficient published data concerning the oil production trends experienced in the field. It is hypothesised (from the above former numerical studies) that reducing the air injection rate will lead to lower oil production rates. On the other hand, Wei et al. (2020) carried out a detailed analysis of the Kerrobert THAI field data including air injection and oil production rates. Their findings can be summarised as the following: 1. there is no clear relationship between air injection and oil production rates, 2. more air injection into the reservoir does not promote higher oil production, which is related to combustion zone development, 3. higher gas saturation caused by excessive air injection increases gas relative permeability which hinders the oil production, and 4. higher air injection promotes greater cooling of system. Their analysis was purely based on analysing field data and no simulation work was carried out to explore the dynamic mechanism of the THAI process. A more detailed investigation of the oxygen utilisation, and its effect on the THAI performance, has been recommended by other workers in order to study how other real reservoir factors such as bottom water may impact the overall stability of THAI process.

This research focuses on the operational aspect of the THAI process. This work, for the first time, presents a field-scale THAI model that was validated against data obtained from the Kerrobert THAI project. The model includes the existing relatively thick bottom water in the studied formation. The first aim of this study is to determine whether variation in the air injection rates can promote the oil production rates during the THAI operation. It is highly likely that excessive air injection causes reduction in oxygen utilisation throughout operation. This means the ISC overall performance will be compromised if improper volume of air is injected into the reservoir (for the sake of higher oil recovery). A secondary aim of this study is to numerically develop and test scenarios for optimisation purposes. A real life quasi-staggered line drive (QSLD) THAI well configuration (namely the K2 THAI well pair in the Kerrobert project) is studied in this work. The potential outcomes of this research are that it could improve the understanding of operational aspects of the THAI process and enhance recovery efficiency of the process for the forthcoming projects.

2. Field data analysis

Primary oil recovery of 1.5% was achieved in the Kerrobert field, located in Southeast Saskatchewan, Canada. This low production has been linked to high viscosity of the oil and presence of bottom water, which leaves a significant amount of resource left for secondary recovery/enhances oil recovery (EOR) schemes. Many operators in Western Canada employ thermal methods to recover remaining heavy oil in the reservoir after primary extraction has become uneconomic (Wikel and Kendall, 2012).

The Kerrobert THAI project is located at the Waseca Channel, Saskatchewan. The geological setting and stratigraphy of the Waseca sandstone formation were investigated by Hill (2017). The Waseca reservoir is a fine-grained sandstone reservoir with depth to the top of the formation varying between 758 and 774 m (oil-water contact is at 789). Oil zone thickness is 12–20 m in the Western part and increasing up to 25–30 m in the Eastern part. The depth of bottom water is approximately 20 m in the Western part and around 10 m in the Eastern part (Turta et al., 2018).

There were several old legacy horizontal wells in the area prior to the THAI project. The old horizontal wells are marked as 1 to 9, in order, starting from the south-east corner in Fig. 1. The THAI project consists of 2 pilot well pairs (WPs) (denoted K1 and K2) and 10 semi-commercial WPs (denoted K3–K12) within Eastern and Western pads (shown in Fig. 1). The operation started with pilot WPs in 2009. The semi-commercial wells were drilled in 2011 (Wei et al., 2020).

Fig. 2 shows a schematic of the Kerrobert THAI project. The vertical air injector well (2) was placed near the toe section of the horizontal production well (1) that was drilled at the base of the reservoir. Following a steam preheat period (pre-ignition heating cycle (PIHC)), air was injected to initiate combustion (3). The vertical combustion front broadens and moves horizontally through the reservoir from the toe of the production well to the heel (4). The heat generated reduces the viscosity of the heavy oil in the mobilised oil zone (MOZ) ahead of the combustion front and enables it to flow by pressure gradient and gravity drainage into the horizontal production well (5). The oil flows to the surface plant facilities where it is treated and sent to market (6) (Petrobank Energy and Resources Ltd, 2012).

The K2 pilot THAI well pair was placed at the Eastern part of the Kerrobert formation. The K2 well pair consists of KA2 and KP2, denoting the vertical injector and horizontal producer wells, respectively. Both KA2 and KP2 were favourably positioned as they were located relatively far from any of the old wells in the region. Therefore, no external interference in K2 pilot operations was expected from the old wells. The K2 well pair was considered as the ideal THAI pilot. This was due to its quasi-staggered line drive (QSLD) well arrangement (shown in Fig. 1). Fig. 1 shows that the lateral distance between the injector well and the horizontal section of producer well (Id) is 12–15 m, and that from the toe to the line of injection (dt-il) there is a distance of 8–10 m. The lateral well spacing between horizontal producers is 70–90 m, while the lengths of the horizontal sections are 400–450 m. The closest injector well to KA2 is KA5 (which belongs to K5, one of 10 semi-commercial THAI well pairs that were drilled and operated later). The KP2 well has its horizontal section located towards the top of the pay zone to minimise water production. There were 20 thermocouples installed in the KP2. Progressive cavity pumps (PCP) were installed in the heel region of KP2 for artificial lifting of heavy oil (Turta et al., 2018).

The operational history of the Kerrobert THAI project is available in a study by Wei et al. (2020). The K2 pilot operation started with the PIHC in September 2009. Cumulatively, 3132 m^3 steam was injected for 51 days via KA2 (the steam injection rate was 62 m^3/day on average). The air injection began in late October 2009. The initial air injection rate was 5000 m^3/day, with a projected maximum injection rate of 80,000 m^3/day. The in-situ combustion front was generated relatively slow in the K2 pilot. The ignition delay was up to 1–2 months. The quality of ignition was very good. The ISC behaviour of K2 was in a toe-to-heel propagation fashion. The ISC toe-to-heel propagation did not take place in the case of K5 (neighbouring semi-commercial THAI well pair) and a combustion chamber around the toe of KP5 was developed. It is believed that the KP5 combustion chamber has influenced the K2 pilot overall performance, which will be discussed later in this paper.

Fig. 3 shows the daily air injection and oil production profile for the K2 THAI pilot well pair from Nov. 2009 to May 2016 [dataset] (Petrobank Energy and Recources Ltd, 2021). A wide range of air injection rates were tried for K2 during the first year of the project. The project's operator did not rely upon any numerical model and the air injection profile was mainly based on trial and error. The air injection rates were larger in late 2009 and 2010 (up to 85,000 m^3/day in August 2010). The operator had to reduce air injection rates because temperatures as high as 1100 °C were observed at the toe section of KP2. It must be noted that the maximum operating temperature for KP2's instrument string was 1200 °C. In addition, initial high injection rates led to surges of gas

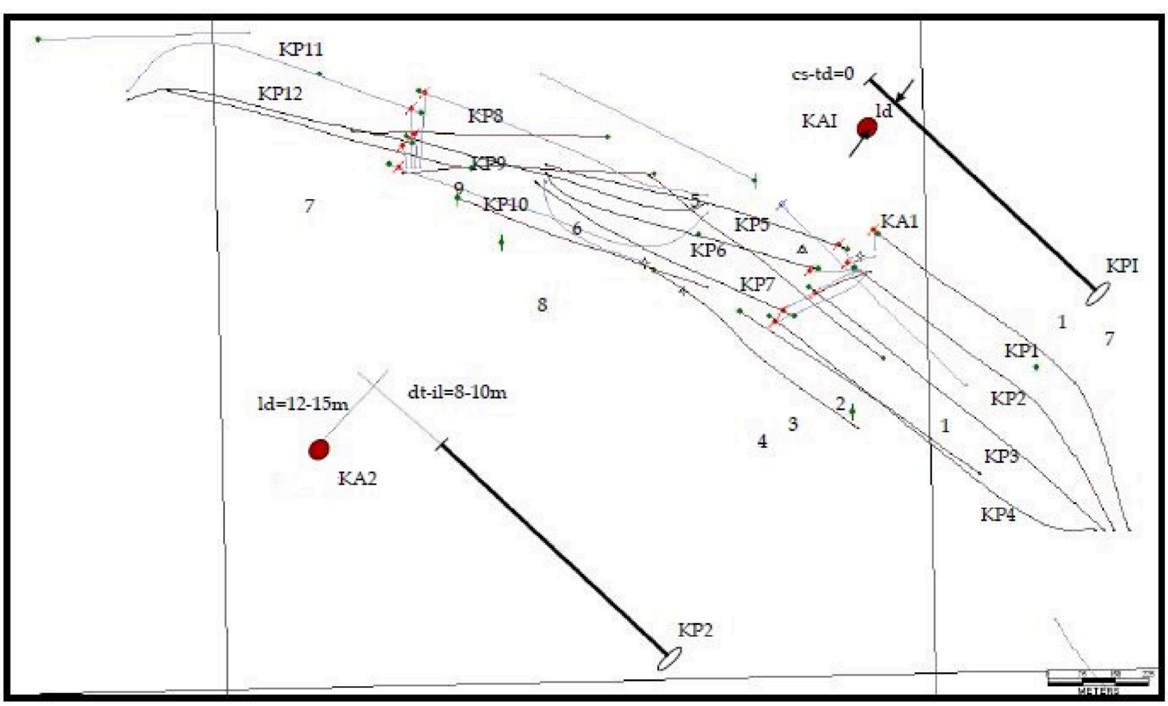

Fig. 1. The location of THAI well pairs (K1–K12, where KA is vertical injector and KP is horizontal producer). Old horizontal wells are marked from 1 to 9 (Turta et al., 2018).

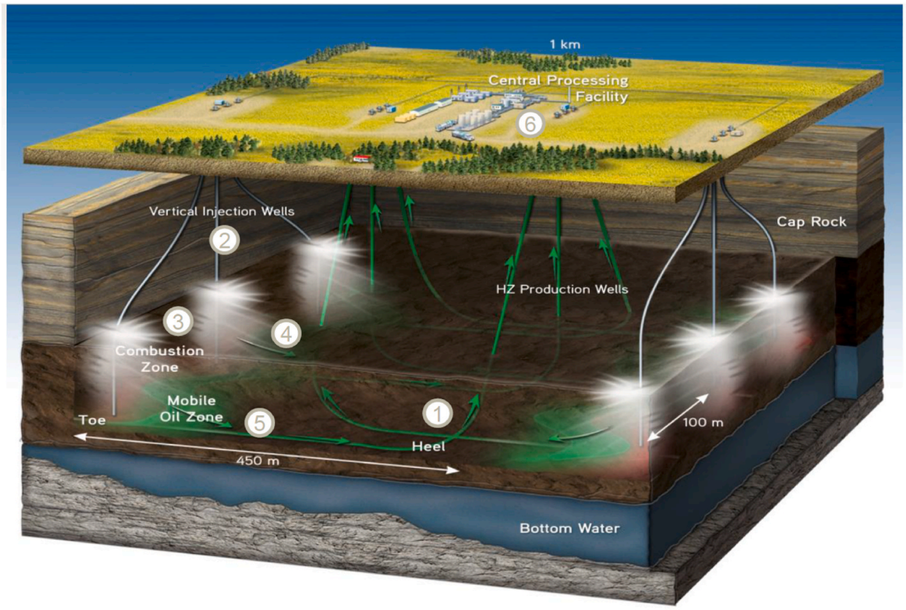

Fig. 2. Schematics of the Kerrobert THAI project (Petrobank Energy and Resources Ltd, 2012).

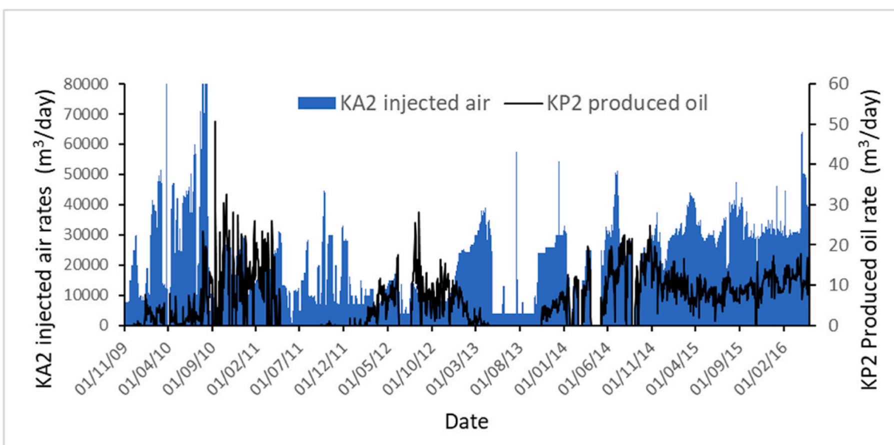

Fig. 3. K2 air injection and oil production profiles.

production from KP2 (which could not be handled by the operator at the surface properly). Consequently, the oil production trend was not consistent for the initial stage. However, daily oil rates up to 25 m^3/day were recorded in late 2010, implying the potential of THAI process.

The air injection rates were not primarily varied to improve the oil production rates during the THAI operation in the K2 case, according to Petrobank. The decision-making regarding change in air injection rates was based on the following criteria in order of importance:

1. Ability of the production pumps to handle a high gas factor (>500 GOR), temperature (around 170–200 °C), and sand content (>2%) in the flow
2. Downhole temperatures (900 °C was a limit for the integrity of the wellbore)
3. Handling produced gas from KP2 at the surface (depending on the gas production rates, the surface temperature can be relatively high)

The KP2 well was down many times in 2011. The operational interruptions were mostly related to pump changes and issues with downhole equipment due to high temperatures. Eventually, the long instrument string was repaired in 2011, meaning no production from late-April 2011 to mid-Feb 2012. Nevertheless, the air injection into KA2 was not stopped while KP2 was down. This was because of concerns regarding the advancement of the in-situ combustion front. The air was injected in order to maintain the combustion front while the producer well was down. The KA2 air injection rates were between 4000 and 20,000 m^3/day in 2012. The reduction in air injection rates was in conjunction with the preparation of the neighbouring semi-commercial K5 THAI well pair. Despite low injection rates, the daily oil production remained in the range of 3–16 m^3/day. The KP2 well was down due to operating issues from April to September 2013. Likewise, the air injection was not stopped then either due to the aforementioned reasons.

The benefits of having a steady or constant oil production profile are: (a) the income stream is maintained at a high level and (b) use of surface facilities is more cost efficient (Greaves et al., 2012 a). The operator had a better understanding of THAI performance from late 2013, allowing for less operation-caused fluctuations. The injected air profile was more stable (on average 25,000–30,000 m^3/day) and it was not interrupted from September 2014 to May 2016. Consequently, good/steady oil production rates were achieved. 6067 m^3 oil was produced in 590 days of operation (in average 10.3 m^3 per day).

Fig. 4 shows the air injection profile, cumulative air injected, gas

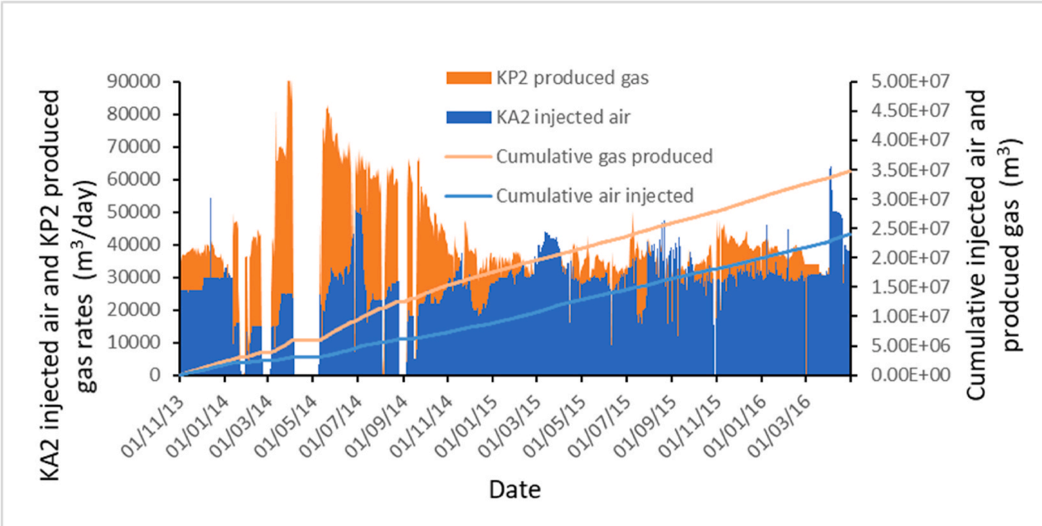

Fig. 4. The air injection profile, cumulative air injected, gas production profile, and cumulative gas produced for the K2 (form November 2013 to April 2016).

production profile, and cumulative gas produced [dataset] (Petrobank Energy and Recources Ltd, 2021). The cumulative volume of produced gas by KP2 is compared with the cumulative volume of air injected into KA2. The cumulative volume of produced gas from KP2 is 30% higher than the cumulative air injected into the corresponding injector well (KA2). Previously, it was assumed that the 30% additional produced gas is made up of hydrocarbon gas injected into KP2 annulus (mainly methane to mitigate corrosion) (Turta et al., 2018). This conclusion, however, was not verified at the time.

The imbalance between the cumulative air injection and gas production for K2 is too high to be neglected. It is thought that K2 has experienced interference from K5, which is the closest neighbouring THAI well pair to K2 at the Eastern part of Kerrobert project. The likely well-to-well interference is because of the very short distance between KA5 and KP2 and the fact that the air injection into KA5 developed a combustion chamber around the toe section of KP5 (instead of toe-to heel propagation). Therefore, some of the KA5 injected air might have been channelled towards KP2. It is difficult to approximate the exact channelled air volume flowing from KA5, but it is considered reasonable that the extra 30% produced by KP2 can be taken as a rough estimate. The good oil production profile (shown in Fig. 3) achieved could reflect the combined contribution of air injection from both KA2 and KA5.

Hence, the interaction between neighbouring air injectors must be considered for a successful prediction of the performance of a THAI project, and this can validate previous speculation. This will be investigated here using a history-matched THAI numerical model. The new field-scale THAI model, for the first time, considers a relatively thick bottom water layer. The effect of air injection rates on the overall efficiency of the THAI process in the presence of bottom water will be explored in this paper. It will be shown that achieved oil production rates can be significantly improved (36% cumulatively) by employing an appropriate air injection profile during the THAI operation. The effect of oxygen utilisation on the various zones developed during the ISC will be studied numerically. The location of the horizontal producer will be examined to enhance the THAI performance in the Kerrobert project. It will be seen how the well-validated field-scale model can be used to investigate scenarios for more efficient operation.

3. THAI simulation

3.1. Model development

The STARS software, developed by Computer Modelling Group (CMG), was used for this study. STARS is a three-phase multi-component thermal and steam additive simulator. ISC simulations are sensitive to grid block size. Ado (2020 a) carried out a study on the effect of the grid system on THAI simulation. The grid system used in this study (shown in Table 1) is based on a grid design for the field-scale THAI simulation studied by Ado (2020 a) (Model P).

The reservoir model is a regular Cartesian grid (with 45, 19, 11 blocks in the i, j, and k directions, respectively). The original grid blocks were then split into 3 refined grid blocks in the i direction, and 3 refined blocks in the j direction. The original grid blocks were not refined in the k direction. Grid refinement was not conducted for the gird blocks in which the vertical injector (VI) and horizontal producer (HP) wells were located. The aim of the grid refinement was to provide a better flood front resolution and reservoir description. The properties of the fundamental blocks were transferred to the corresponding constituent refined grid blocks. A single porosity type was assigned for the formation. The sink/source well model was used for both VI and HP. Only the horizontal section of the horizontal producer well was perforated. Aquifer modelling (bottom water section) was done by adding cells that contain only water. Fig. 5 represents the dimensions of reservoir model and quasi-staggered line drive (QSLD) well arrangement of the K2 pilot. The model consists of three main sections (namely the pay, transition, and bottom water zones) based on their fluid saturation (shown in Fig. 5). The simulation was made for a homogenous oil layer. No steam was injected into the reservoir model prior to air injection. An electrical heater was used to preheat the inlet zone (around injector well) of the reservoir and to bring it up to ignition temperature.

3.2. PVT and petrophysical properties

Athabasca heavy oil pressure, volume, and temperature (PVT) data, reported by Ado et al. (2017), were used for this study. They defined LC, MC, and IC as the Light, Mobile, and Immobile pseudo-Components, respectively. Likewise, the molecular fraction, temperature-dependent viscosity, and equilibrium *K*-values for each heavy oil pseudo-component have been taken from the study by Ado et al. (2017).

Table 1
Grid block refinement system.

Reservoir Dimension (i × j × k)	220 m × 100 m × 38 m
Number of original grid block (i × j × k)	45 × 19 × 11
Number of refined grid block (i × j × k)	135 × 57 × 11
Total number of grid blocks	91,782

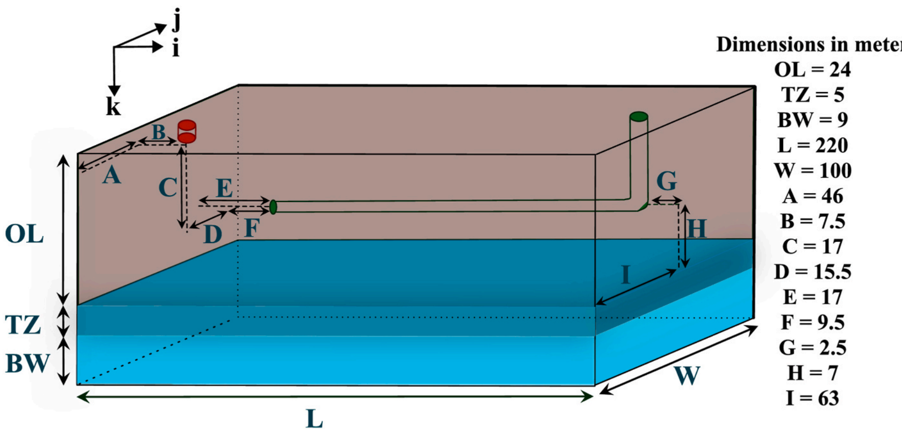

Fig. 5. Reservoir model dimensions and VI and HP configuration in quasi-staggered line drive (SQLD) fashion. Notes: *The oil layer (pay zone), transition zone, and bottom water zone are shown in grey, dark blue, and light blue, respectively. (For interpretation of the references to colour in this figure legend, the reader is referred to the Web version of this article.)

Water (steam), oxygen, inert gas (CO_x), and coke were the other four components in the model. The petrophysical properties used for this study are shown in Table 2 (taken from studies by Turta et al. (2018) and Wikel and Kendall (2012)). The oil/water and gas water relative permeability curves are based on rock-fluid data by Ado et al. (2017).

The composition of air injected into the reservoir, as well as its injection pressure and temperature, are shown in Table 3. A minimum bottom hole pressure and a maximum surface liquid rate were also set as the horizontal producer constraints.

3.3. Kinetics scheme

Ado (2020) used a new upscaling procedure to carry out a comparative study between the predictions for two different types of validated kinetics schemes. Two models (model P and G) were proposed. The kinetics scheme used for Model G was heavily dependent on the stoichiometric coefficient of the product of the reaction. It was concluded that model P provided a more realistic prediction of the THAI process. Model P employed a direct conversion thermal cracking scheme together with the combustion reactions for field-scale THAI modelling. Another merit of model P was to include low temperature oxidation (LTO) reactions as well as high temperature oxidation (HTO) reactions. Table 4 a and b present similar THAI kinetics to those proposed by Ado (2020), with minor adjustment, that was used for this study. The default setting of the STARS software was used in order to calculate the enthalpies of the thermal cracking reactions. The heats of reaction for the combustion reactions were taken from the study by Ado et al. (2017).

4. Model validation by history matching

In this section, two models (Model S and D) were constructed using the actual field data from the Kerrobert THAI project. Both Model S and D used the same physical properties as described earlier in Section 3.1. Model S was history matched and validated against the K2 THAI pilot well. Model D was built to investigate the effect of variation in air injection rates on the overall performance of the THAI process in the presence of bottom water.

Table 2
Properties and initial conditions of the Eastern Kerrobert reservoir.

Reservoir porosity		0.32	
Horizontal permeability, k_h (mD)		4948	
Vertical permeability, k_v (mD)		3793	
Initial reservoir temperature (°C)		20	
Initial reservoir pressure (kPa)		3000	
Dead oil viscosity at reservoir temperature (mPa.s)		33,491–89,000	
Live oil viscosity (mPa.s)		>21,000	
The asphaltene content		14%	
Reservoir zones	Pay zone	Transition zone	Bottom water zone
Initial oil saturation, S_{oi}	0.74	0.55	0
Initial water saturation, S_{wi}	0.26	0.45	1
Initial gas saturation, S_{gi}	0	0	0

Table 3
Injected air properties and production well constrains

Injected fluid composition (%)	Injected fluid pressure (kPa)	Injected fluid temperature (°C)	Production well minimum bottom hole pressure (kPa)	Production well maximum surface liquid rate (m^3 day^{-1})
CO_x (79) & O_2 (21)	3500	25	3000	300

Table 4
a and b. THAI Kinetics scheme. Note*: IC is Immobile pseudo-Component, MC is Mobile pseudo-Component, and LC is Light pseudo-Component.

a. Thermal cracking reactions	Frequency factor (min^{-1})	Activation energy (J $mole^{-1}$)
IC → 2.0471 MC	6.4726×10^{15}	239.01×10^3
MC → 0.4884 IC	5.7004×10^{13}	215.82×10^3
MC → 2.3567 LC	1.9171×10^{10}	184.88×10^3
LC → 0.4243 MC	2.5809×10^{10}	180.45×10^3
IC → 77.4563 Coke	3.9289×10^{10}	180.88×10^3

b. Combustion reactions	Frequency factor (min^{-1} kPa^{-1})	Activation energy (J $mole^{-1}$)	Heat of Reactions (J $mole^{-1}$)
IC + 106.68 O_2 → 83.32 CO_x+ 46.90 H_2O	3.0686×10^5	138×10^3	4×10^7
MC + 37.06 O_2 → 29.74 CO_x+ 22.36 H_2O	3.0686×10^6	138×10^3	1.6×10^7
LC + 17.46 O_2 → 11.81 CO_x + 14.5 H_2O	3.0686×10^7	138×10^3	4.91×10^7
Coke + 1.22 O_2 → 0.97 CO_x+ 0.565 H_2O	1.6935×10^7	123×10^3	3.9×10^7

4.1. Modelling K2 THAI pilot

Geostatistical models built with static data only tend to give a very wide range of production profiles, but utilisation of dynamic data, such as production rates, will more substantially constrain a model (Baker et al., 2006). A direct comparison between the KA2 air injection rates and the KP2 gas production rates (shown in Fig. 4), suggests that a THAI model successfully matching air injection and oil production profiles is not reliable unless it considers the gas production profile. Petrobank reported that the imbalance between cumulative air injection and gas production in the K2 pilot was most likely caused by interference with its neighbouring semi-commercial THAI well pair (K5). This was possible due to the short distance between K2 and K5 well pairs (shown in Fig. 1). Hence, the produced gas rates for KP2 must be assumed as contributing to air injection rates for KA2 for history matching purposes. This is to incorporate the effect of extra air from KA5. Henceforth, the history matching model is referred to as Model S in this work. The data of particular interest for Model S was from November 2013 to April 2016, since minimal operational interruptions occurred during this period. No steam was injected into the reservoir model prior to air injection.

Fig. 6 provides a comparison of simulation results from model S with field data from the K2 THAI pilot. Apart from the initialisation period, the developed model was able to replicate daily oil production closely. The initial deviation in oil production rate between the predicted result and field data is due to: a. the communication between injection and production well was achieved 50 days after commencing air injection in Model S, which led to a short delay in oil production. It must be noted that the K2 pilot well pair was operating and producing oil prior to the simulated period, b. the higher initial oil production in Model S compared to field data is due to the pressure build up in the model before the establishing of communication between injection and production wells. However, good agreement was achieved for daily oil production rates from late January until mid-July 2014. The simulated produced oil rates were slightly lower than field data from mid-July to early-December 2014. This was due to a change in oxygen utilisation in the model, which will be discussed when the combustion front is considered in detail in Section 5.2 later in this paper. The simulated oil production rates tracked field data quite closely from early-December 2014 onwards. This narrowed the earlier difference between simulated cumulative oil production and field cumulative oil production data (final agreement within 3%).

The good performance of K2 in terms of the oil production is a clear indication that a strong in-situ combustion front had occurred. It is plausible that temperatures higher than 800 °C were generated (Turta et al., 2018). Substantial data were generated by 20 thermocouples, which were placed along the horizontal section of the KP2 well (5 of them within 15 m from the toe and the remainder at the larger intervals up to the heel). Fig. 7 shows the variation in temperature along KP2 from Jul 2011 to Nov 2016. Thermocouples located at the toe region of KP2 experienced a very high temperature, leading to their failures. Model S, as shown in Fig. 8, predicted high temperatures up to 650 °C within 15 m of the toe section of the HP too. Similar to seen in the field data, a lower range of temperatures was observed around the perforations closer to the heel of the HP well in Model S. The simulation results showed excellent agreement with the temperature profile for the toe section between July 2014 to January 2015.

4.2. Effect of additional air ingress from KA5 on overall performance of K2

A recent field data analysis by Wei et al. (2021) suggests that more air injection does not promote higher oil production. Their analysis was purely based on field data and no simulation work was carried out to explore the dynamic mechanism of the THAI process. A constant air injection rate of 20,000 m^3/day was used for a THAI numerical study by Ado (2019). Araujo et al. (2016) reported results for different continuous air injection rates from 0 to 40,000 m^3/day for their simulations. They reported a maximum limit of air injection of 35,000 m^3/day for their THAI models with thickness of 26 m (oil zone of 20 m and water zone of 6 m). However, both previous THAI numerical studies with BW were not validated against field data. In the present study, the history-matched simulation (Model S) was used to numerically investigate the effect of air injection rates on THAI performance in the presence of bottom water. A new model is designated as Model D, and consisted of the restriction of air injection to only that into KA2 alone itself (hence, injected air rates were lower compared to Model S). The physical and petrophysical properties of Model D were the same as for Model S. No steam was injected into the reservoir model prior to air injection.

Fig. 9 shows a comparison of the simulation results from Model D with field data from the K2 THAI pilot. The oil production started after 130 days of air injection, in early March 2014. Oil production was delayed for 70 days compared to Model S results. This indicated that it takes a longer time for oil to become mobile and drain into the HP well when it is subjected to lower air injection rates. A sharp peak in oil production was observed at the initial stage, which was in line with field

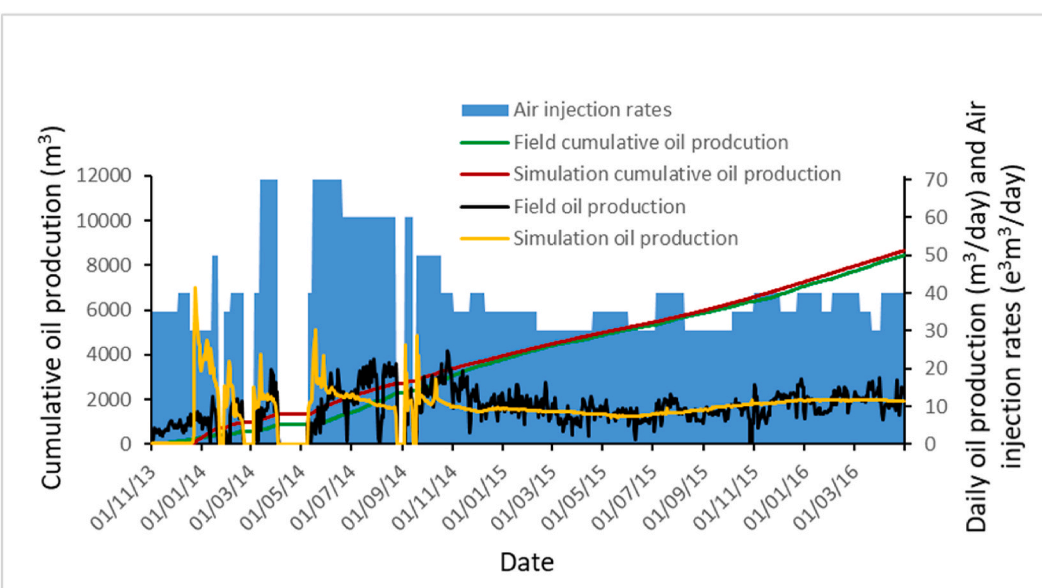

Fig. 6. Comparison of simulation results for Model S with field data for the K2 pilot.

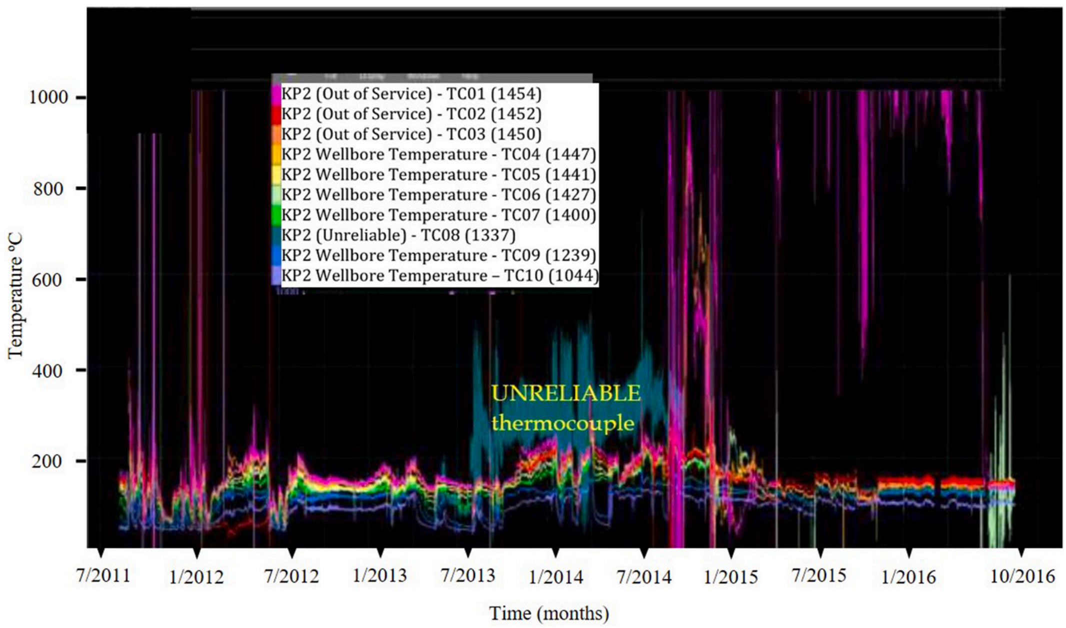

Fig. 7. Actual variation of temperature along KP2 versus time. Notes: * TC01 is located at the toe of HP.

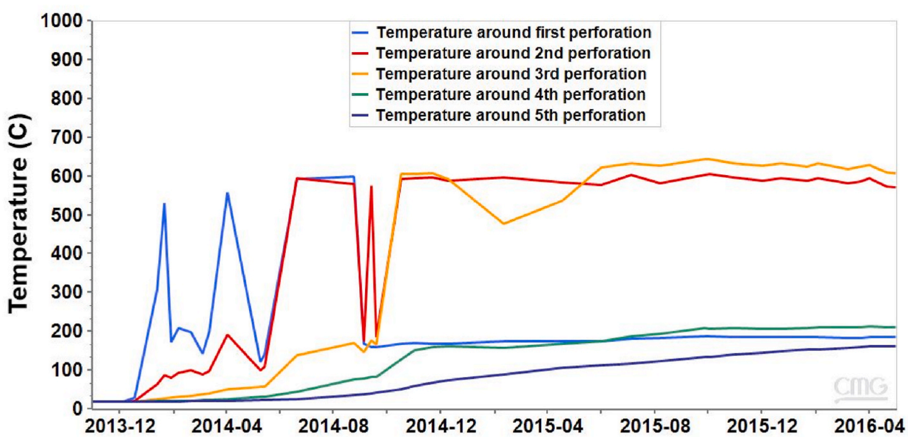

Fig. 8. Predicted variation of temperature around the toe section of HP in model S against time. Notes: * Order of perforation is from the toe side of HP.

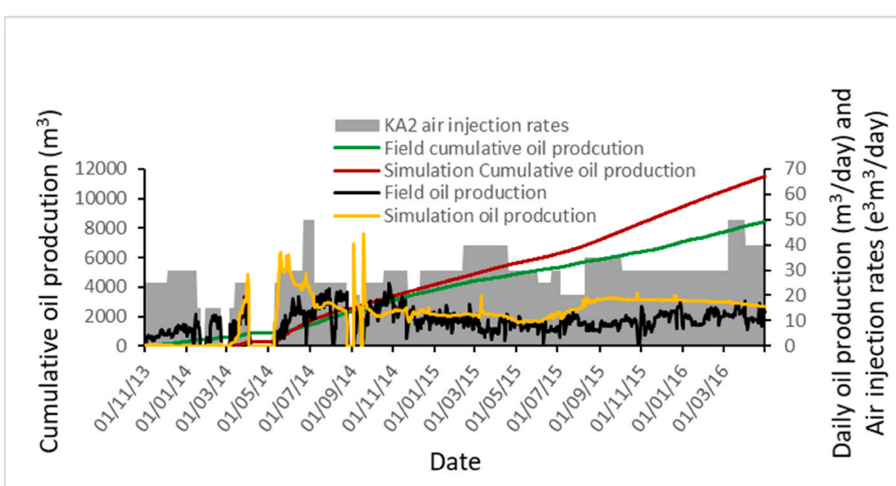

Fig. 9. Model D simulated oil production profile compared with corresponding field data for K2.

data. However, Model D predicted higher oil production (up to 35 m^3/day) compared to field data after reopening the producer well in early May 2014. This was due to the pressure built up around the toe section prior to the closure of the HP. The simulated oil production rates declined from early-July to late-August 2014. Oil production rate was even lower than field data before HP closure in late-August 2014. The simulated oil production time series was higher than field data during the uninterrupted K2 operation period (early-Sep 2014 to May 2016). The final cumulative oil production predicted by model D was 36% higher than K2 field data and 33% higher than Model S results, respectively. The predictions from Model D in the present study are consistent with the suggestion previously by Wei et al. (2020) and Araujo et al. (2016), namely that more air injection into the reservoir does not promote higher oil production. On the other hand, Fig. 10 shows simulated water cut against air injection rates for Model S and Model D. The predicted water cut profile for history-matched model (Model S) was in line with field data reported by Turta et al. (2018). They reported that water cut decreased from 70–90% to as low as 30–50% for the KP2 well. The earlier oil production reduced the water cut in the produced fluid in Model S at an earlier stage of the THAI process. However, the predicted results (from mid-May 2014) show that excessive increase in air injection rates led to an increase of water cut in Model S compared to model D.

5. Results and discussions

In this section, simulation results from both Models S and D are examined. The effect of air injection rates on the overall performance of the THAI process will be studied. Detailed analyses are carried out for all the distinct zones established during the THAI process. Greaves et al. (2012b) proposed a schema consisting of a series of zones that develop during the steady-state operation of the THAI process when the combustion front propagates from the inlet end to the production end of the reservoir (shown in Fig. 11). The zones that were developed during the in-situ combustion (ISC) process include:

A. Combusted zone, the area that has already been in contact with the combustion front. All the oil has been displaced, meaning that there is only clean sand in there.
B. Combustion zone, the leading edge of combusted zone where the oxygen is completely consumed.
C. Coke zone, the area that coke (a product of thermally cracked heavy oil) is deposited ahead of combustion front.
D. Steam zone, the water supplying this zone comes from the resident reservoir water and from the combustion reactions.
E. Mobile oil zone, this area contains two regions; (region 1) thermally cracked oil as well as lighter vaporized fractions and (region 2) banked oil zone where the oil saturation is close to 100%.
F. Cold oil zone, this area contains the original crude oil.

The proposed schema by Greaves et al. (2012 b) was based on an experimental scale THAI simulation. It must be noted that their experimental scale model did not consider a bottom water zone. Major developed zones in the THAI process (as outlined above) in presence of bottom water will be probed using the history matched field-scale THAI simulation (Model S) in this section. The predictions from Model S and Model D (that excludes the additional air ingress from KA5) will then be compared. This comparison is to study the effect of including extra air ingress from KA5 on the developed zones during the THAI process. 3D, areal and cross-sectional views were used for the following investigations.

5.1. Combusted zone (swept region)

Fig. 12 (a) shows a 2D simulated ternary oil-water-gas profile for Model S (top) and Model D (bottom) in May 2016. The region (in red) with 100% gas saturation in the ternary profile is a good proxy indicator of the combusted zone. The oil initially in the inlet zone of the reservoir was swept by the combustion front, leaving only clean sand behind. It is evident that the combusted zone is larger in Model D compared to Model S. However, comparing the Model S and D ternary profiles, the combusted zone shapes were approximately similar. In contrast, the swept zone for Model D was more advanced into the reservoir (particularly, at the first and second top horizontal planes). Similarly to the past THAI field-scale simulations by Greaves et al. (2013) (i.e. 25 m pay zone case), the combusted zone was mainly restricted to the inlet section leading to the toe section of the HP. Good volumetric oil sweep, with uniform oil displacement, can be identified across the inlet section of the reservoir for both Models S and D in Fig. 12 (b). Temperatures as high as 600 °C were predicted at the toe section of the HP for both models (mostly during the uninterrupted air injection period) (shown in Fig. 8). This high temperature is related to the extensive gas saturation in the region. The grid block became nearly fully saturated with hot gas, thereby resulting in the prediction of elevated temperatures. The relative permeability of the oil phase dropped to zero as the large amount of air in the reservoir pushed the oil away from the producer. A similar event was reported by Wei et al. (2020). Additionally, the simulation indicated that some oil sank into the bottom water zone (shown in both Fig. 12 (a) and (b)). The mobilised oil replaced some of the water originally in place in the bottom water area of the reservoir. This will be investigated in detail here later in Section 5.5.

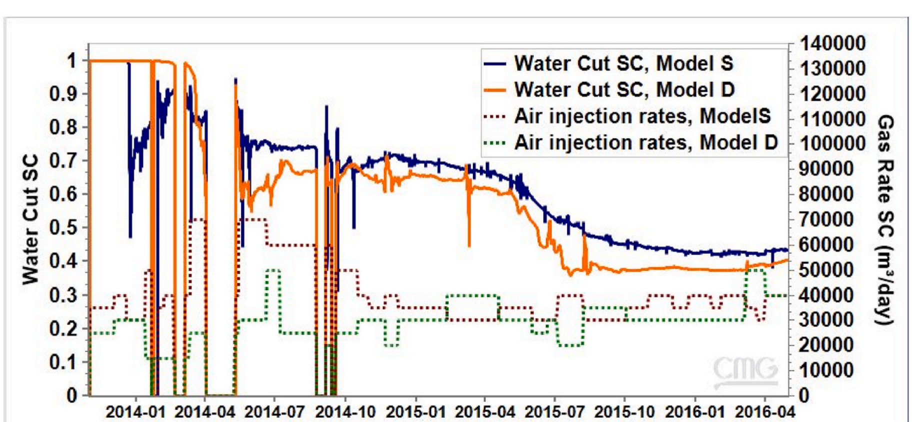

Fig. 10. Simulated water cut against air injection rates for Model S and Model D.

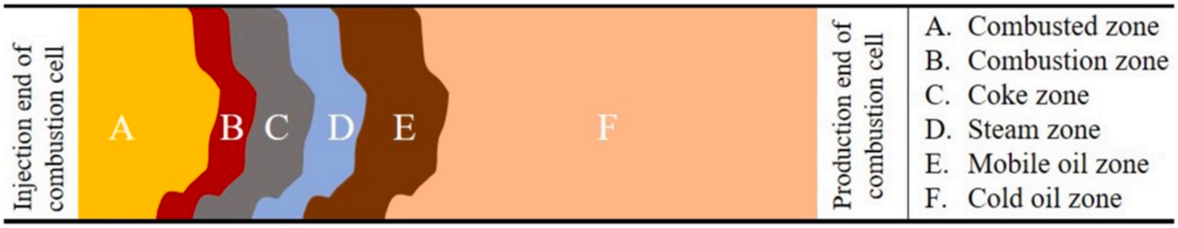

Fig. 11. Areal schematic of zones developed in the THAI process.

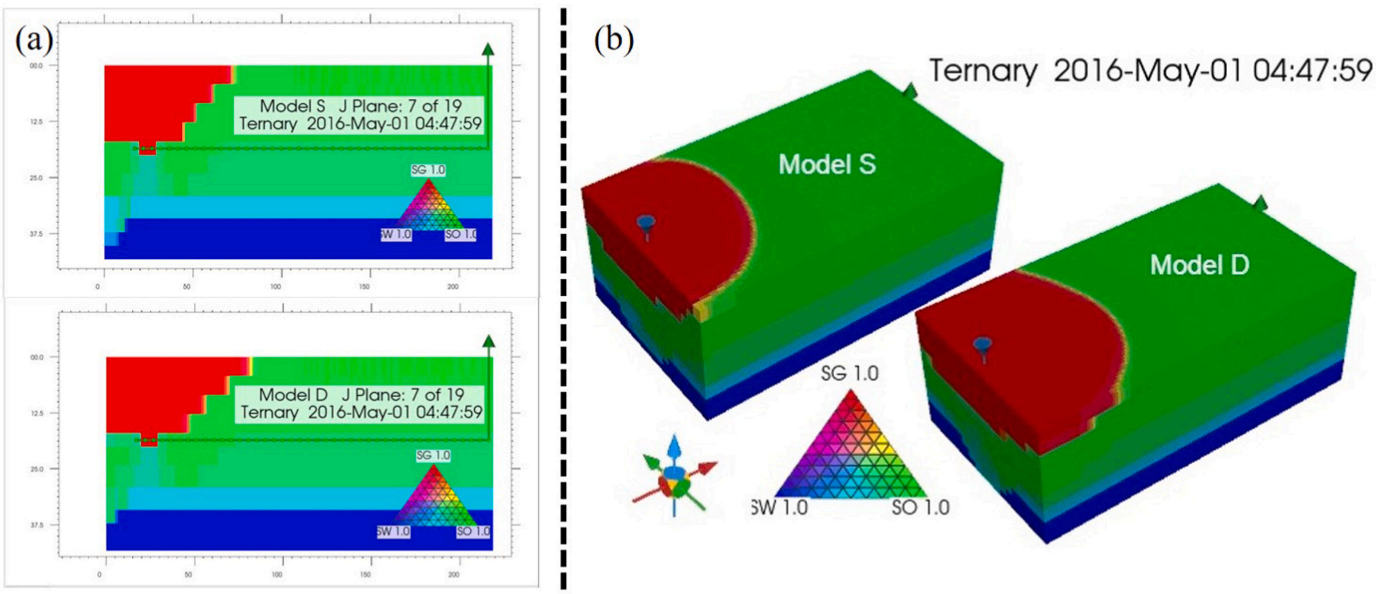

Fig. 12. Simulated ternary profile for model S and D in vertical midplane view (a) and in 3D (b) in May 2016. Notes: * SO, SW, and SG represent oil saturation, water saturation, and gas saturation, respectively.

5.2. Combustion zone

Fig. 13 shows the predicted oxygen profile for both models (Model S on left side and model D on right), during November 2014, July 2015, and May 2016. The oxygen profile is an accurate proxy representation of the combustion front shape. This is because, at the leading edge of the combustion front, the O_2 concentration drops to zero, and this is coincidental with the leading edge of the oxygen front (Greaves, et al., 2012 b). The region behind the combustion front (combusted zone) was occupied by the injected air. Comparing the oxygen profile for both models in Fig. 13 (a), it can be observed that the combustion front was already touching the toe section of the HP in model D in Nov 2014, whereas no O_2 was in the vicinity of the toe section of the HP in model D at the same time. This is due to higher air injection rates in the history-matched model. Thus, the combustion front was more advanced into the reservoir in model D compared to model S in Nov 2014. This is related to the migration of oxygen into the HP in model S and higher O_2 consumption in model D, which will be analysed below in this section. Fig. 13 (b) shows the combustion front expansion in model S and D in July 2015. The same trend in oxygen profile (as in Fig. 13 (a)) can be identified in Fig. 13 (b) for both model S and D, leading to larger horizontal propagation of the combustion front in model D (particularly, the top horizontal layers) in comparison with model S. Simulated results in Fig. 13 (c) shows that the combustion front has a forward leaning shape meaning that a larger areal section was swept by the combustion front at the top of reservoir in both models. Also, Fig. 13 (c) exhibits that the leading edge of the combustion front in model D was in the vicinity of the toe section of HP in May 2016.

Fig. 13 (c, left) shows a vertical midplane of the predicted combustion front for model S in May 2016. High values of oxygen concentration appear to exist around the second and the third perforation from the toe side of the HP. This can be examined in detail by looking at the change in oxygen concentration for the grid blocks in which the toe section of the HP is placed. Fig. 14 shows the variation in the oxygen profile during the THAI process at the first, second and third grid blocks from the toe side of the HP in Model S. Understandably, the shift in oxygen concentration at the toe section of the HP is related to the air injection rates (Fig. 14). The highest oxygen mole fraction around the first perforation of the HP toe section was around 6%, which occurred because of injecting 70,000 m^3/day air into the reservoir in March 2014. As the combustion front propagated along the HP (considering air injection rates of 60,000–70,000 m^3/day from mid-May to mid- Sep 2014), higher oxygen concentrations were detected around the second perforation of the HP toe section (maximum of 9% in September 2, 0,014). There was no oxygen around the first perforation of the HP's toe during the uninterrupted air injection period (air injection rates of 30,000–50,000 m^3/day). Although, a significant concentration of oxygen continued to exist around the second perforation of the HP toe section (maximum of 11% in August 2015). The initial oxygen presence around the third perforation occurred in late-Sep 2014 but it remained below 3% until early-July 2015. However, there was a substantial increase in oxygen mole fraction around the third perforation during last 10 months of simulated THAI process (up to 9% in late-April 2016).

Fig. 14 also shows the predicted oxygen concentration in the produced gas for Model S. It is evident that a high O_2 concentration around the toe section of the HP in model S has caused oxygen channelling into

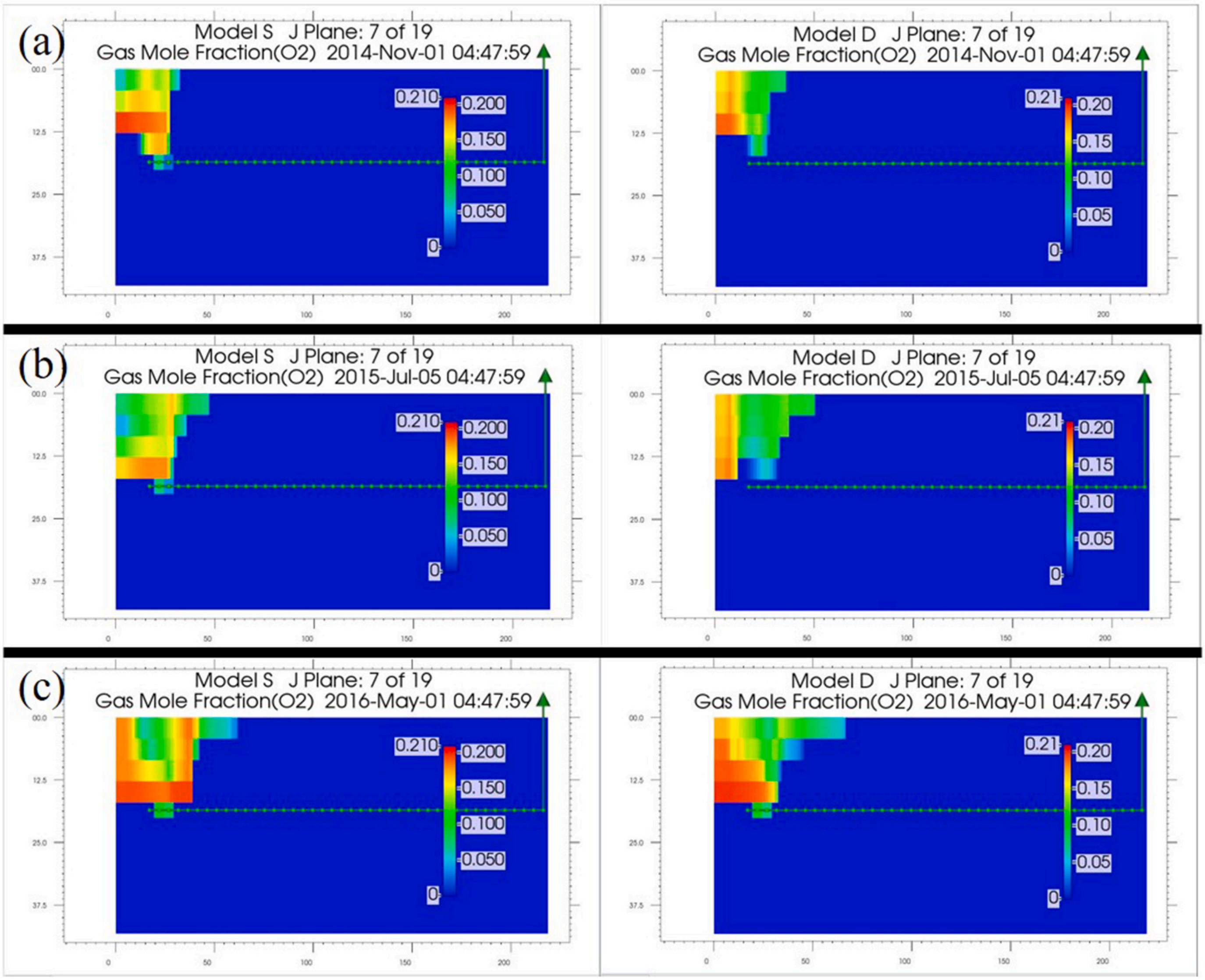

Fig. 13. Change in predicted oxygen profile for Model S (left) and Model D (right) at vertical midplane from November 2014 to May 2016 (uninterrupted air injection period).

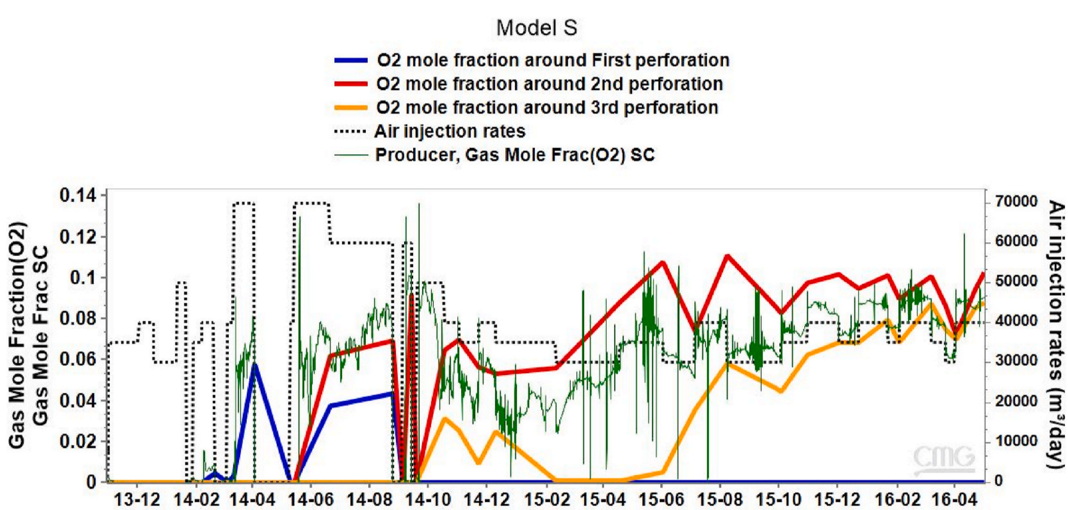

Fig. 14. Variation over time of injected air rates and predicted change in O2 concentration at toe section of the HP by Model S. Notes: * Order of perforation is from the toe side of the HP.

the HP (up to 10%). In contrast, Greaves et al. (2013) reported no evidence from their simulation of any oxygen being produced for the 25 m thick oil layer over nearly 6 years operating period. Further, Greaves et al. (2012 a) predicted breakthrough of oxygen into the production well would occur only after 10.8 years of oil production. However, in both aforementioned previous field-scale THAI simulation studies, the predicted results were for a reservoir model with no bottom water. Additionally, the vertical offset between the injector well and toe section of horizontal producer was around 22 m in both previous studies (5 m longer compared to this work). Moreover, none of the previous field-scale THAI numerical works had been validated against actual field results due to the lack of published data. A more detailed investigation of the oxygen effect has been recommended by other workers, to study how other real reservoir factors, such as bottom water, may impact the overall stability of THAI process.

Unlike the conventional ICS process, THAI is a short-distance oil displacement process with a long zone for the chemical reactions taking place (Turta et al., 2020). The unexpectedly high concentration of produced oxygen in this work can be explained by the particular reactions that may have been taking place in the producer wellbore. Recently, Wei et al. (2020) reported a summary of time-averaged gas composition from each producer well in the Kerrobert THAI project from 2009 to 2015 (shown in Table 5). The recorded produced oxygen from KP2 was only 0.4% (the injected air into KA2 contained 21% O_2 and 79% Nitrogen). They concluded that the low oxygen concentration in the production well was due to either a good combustion within the reservoir or leaving oxygen behind in the reservoir. It must be noted that the oxygen concentrations in produced gas from KP2 does not necessarily correspond to the O_2 profile around the toe section of the HP, according to the Kerrobert THAI pilot operator (Petrobank). The K2 operator confirmed the low O_2 (almost close to zero) production from KP2. However, they recorded problems with downhole equipment corrosion caused by oxygen. The high methane gas concentration in produced gas from KP2 was due to injection of methane to prevent corrosion. Direct oxygen channelling into the production well was also confirmed by the operator when the combustion front was too close to the wellbore. Petrobank was not able to measure downhole O_2 as it was difficult to locate where the inflow point was. It was also expensive to install oxygen sensors and be able to move O_2 sensors closer to/further away from the inflow zone. The assumption was that oxygen and hydrogen reacted within the wellbore and were then produced as water, which cannot be investigated through this numerical work. This is because of a. an absence of H_2 in input components (as well as chemical reactions related to H_2 (coke gasification and water gas shift reactions)) and b. O_2 does not undergo any chemical reaction within the wellbore in the present simulation study. Hence, the excessive predicted O_2 concentration in producer in the present simulation study can be explained. The effect of O_2 utilisation on THAI performance in the presence of bottom water, will be discussed later in this section.

Fig. 13 (c, right) shows the position predicted by model D for the combustion front in the vertical midplane of the reservoir in May 2016. The combustion front has better horizontal propagation at the top layer of the pay zone (around 70 m distance) compared to model S (around 60 m distance). The forward-leaning shape of the combustion front is clearly demonstrated as well. The variation in the O_2 concentration at the first, second and third grid blocks from the toe side of HP, is shown in Fig. 15. Unlike with Model S, the oxygen breakthrough did not occur from the first HP perforation. The dramatic change in air injection rates (to 50,000 m^3/day in early-July 2014) led to oxygen channelling into the second HP perforation, although it amounted to less than 1% in overall comparison. The first significant oxygen breakthrough was seen at the third HP perforation (up to 3% and 7% following air injection rates of 30,000 and 40,000 m^3/day, respectively) from late-Dec 2014 to May 2015). No oxygen was produced from May to September 2015 in response to a reduction in air injection rates to as low as 20,000 m^3/day. Following another air injection rise from 20,000 to 35,000 m^3/day in Sep 2015, the O_2 concentration around the second and third HP perforation increased rapidly. The combustion front was very close to the HP at this point. The uninterrupted air injection accelerated the oxygen breakthrough, and consequently, significant amounts of oxygen channelled directly into the HP through the second and third perforations during the next 7 months.

The impact of the effective oxygen consumption throughout the THAI process was investigated in both models. Fig. 16 shows the data predicted by Model S in red and Model D in green. Comparing cumulative injected oxygen rates, as well as cumulative produced oxygen rates, for Model S and Model D, a higher amount of oxygen was injected into Model S compared to Model D. It is not surprising to see then that the total produced oxygen in Model D is less than Model S. However, the O_2 utilisation by each model is less straightforward. The predicted results show oxygen consumptions of 74% and 90% for Model S and Model D, respectively. It has been mentioned previously, earlier in this section, that the oxygen breakthrough into the HP occurred differently in Model S and Model D. This contributes to the difference in O_2 consumption predicted by Model S and Model D. Looking at Fig. 16, it is apparent that the simulated oil production profile was directly affected by the oxygen consumption throughout the THAI process in both models. This is more noticeable during the uninterrupted air injection period. Apart from two periods of THAI operation (Feb–April 2015 and Mar–May 2016, when excessive air was injected to Model D), the simulated O_2 consumption by Model S was lower than predicted results by Model D. This is a clear indication of better in-situ combustion (ISC) performance in Model D compared to model S. The higher daily and cumulative oil production profile by Model D (shown in Fig. 9) is a direct result of a good overall ISC performance in Model D.

Another indication of poor combustion front propagation in model S can be seen in its temperature profile. Fig. 17 shows the predicted 3D temperature profiles for Model S and Model D in (a) March 2014 and (b) July 2015. High temperature regions can be seen ahead of the combustion front in both models in March 2014. Although, due to inadequate oxygen utilisation in Model S (approximately 70% from Fig. 16), a poor combustion front advancement was predicted for Model S in July 2015. The experimental study by Greaves and Al-Shamali (1996) found that, irrespective of the extent of combustion front established initially, the size of the high temperature region during ISC tends to decrease progressively with increasing combustion time. Because of the higher oxygen consumption by Model D (100% shown in Fig. 16), a high-temperature leading edge of combustion front is still detectable even though it was narrower (in July 2015). This is consistent with findings by Greaves and Al-Shamali (1996). The predicted temperature profile (above 650 °C) shows that the combustion front propagation was more stable in Model D. This implies that the overall ISC performance is directly related to the O_2 consumption during the THAI process.

Both simulated oxygen and temperature profiles by Model S and Model D indicate that selection of proper air injection rates are key for a sufficient oxygen utilisation during the ISC, leading to a successful THAI operation. The findings in this section clearly show that the short distance between the K2 and K5 THAI well pairs, and the subsequent extra air ingress from KA5 towards KP2, have had a negative impact on the performance of the THAI process. Therefore, for forthcoming projects, THAI well pairs must be drilled at a sufficient distance to avoid unwanted interference from each other, unless the operation is based on intended interaction between air injector wells (e.g., staggered line drive (SLD) THAI well arrangement).

Table 5
KP2 average gas compositions from 2009 to 2015 in mole% (HMWG represents high molecular weight gas).

H_2	O_2	N_2	CO	CH_4	CO_2	H_2S	HMWG
1.33	0.40	73.85	0.35	9.26	12.71	0.41	1.10

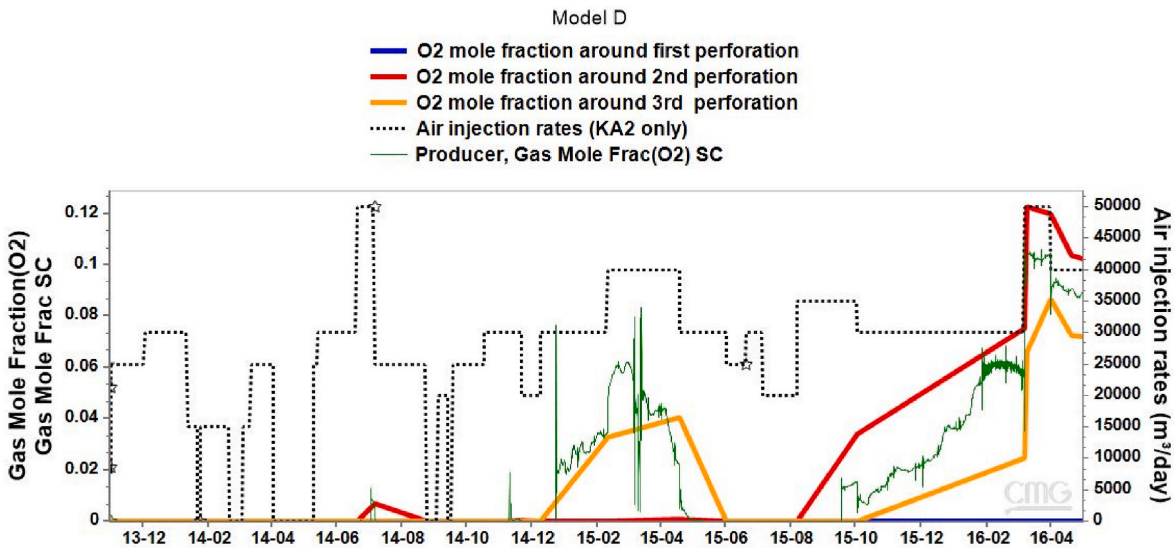

Fig. 15. Variation over time of injected air rates and predicted change in O2 concentration at toe section of the HP by Model D. Notes: * Order of perforation is from the toe side of the HP.

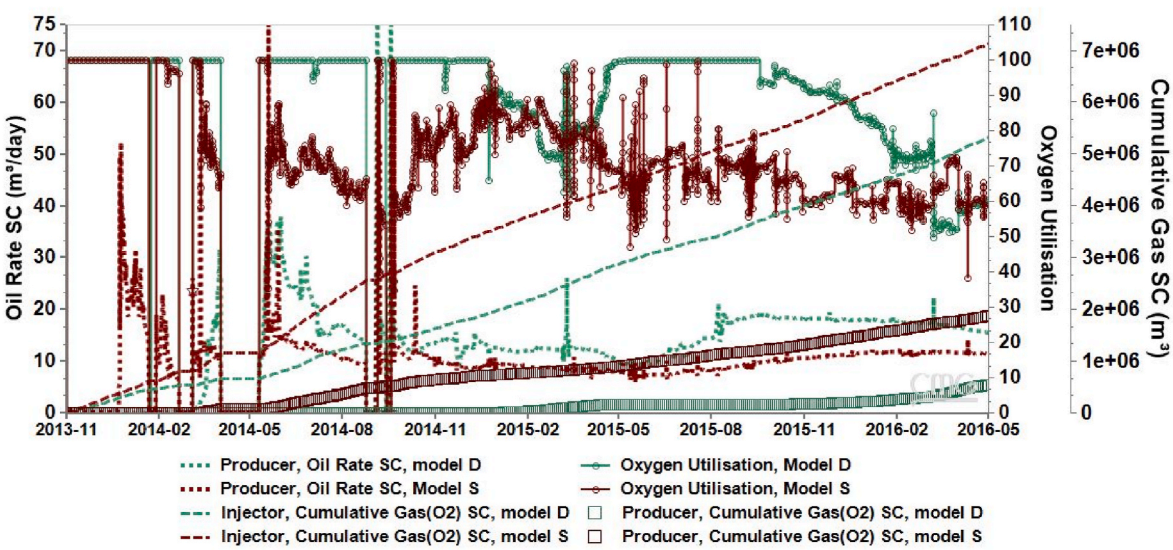

Fig. 16. Cumulative oxygen injected, cumulative oxygen produced, predicted oxygen utilisation, and oil production profile by Model S and Model D. Notes: * The illustrated parameters are distinguished with different line styles.

5.3. Coke zone

The coke zone provides the fuel for the in-situ combustion process. Coke is formed immediately ahead of the combustion front as a result of the precursor processes leading to oil displacement, including vaporisation and thermal cracking (Xia et al., 2003). Fig. 18 shows the structure of the simulated coke zone in 3D for both models S and D. The area swept by the combustion front contained no coke. Coke deposition, with higher concentration (around 500 kg/m^3) and thickness, occurred mainly in the lower part of inlet zone. The highest coke concentration was developed in the transition zone layer in Model S, while high coke concentrations were observed within the HP layer down to the transition zone layer in Model D. In other words, the high coke concentrated zone (displayed in red in Fig. 18) in Model D was larger compared to Model S in May 2016. It can be seen that coke concentration was high at the toe of HP in Model D, which matches the observation of Greaves et al. (2013)(i.e., 25 m thick pay zone reservoir). The heavy oil thermal cracking reactions dominate downstream of the combustion front. This is due to the heat transportation to the base of reservoir via conduction from the reservoir rock, and convection from the mobilised oil zone (Ado, 2020). As the combustion front is limited to the upper portion of the reservoir, the immobile oil originally in place (below the combustion front) has a higher tendency to thermally convert to coke. This resulted in the rise in a higher conversion of heavy oil to coke beneath the combustion front, which is more evident in the predicted coke profile for Model D. A thinner coke zone with lower coke concentration was formed ahead of the combustion front for both models S and D. The average coke concentration ahead of the middle and upper parts of the combustion front was in the range of 50–60 kg/m^3 for both models. The high-performance in-situ combustion in Model D resulted in a uniform coke zone generation ahead of the combustion front. Some instability was identified in the upper part of the coke zone in Model S. The extra air ingress from KA5 caused direct migration of the injected oxygen into the HP in Model S, which consequently led to a reduction in cracking reaction of heavy oil (coke generation).

There was no evidence of oxygen ahead of the coke zone in this

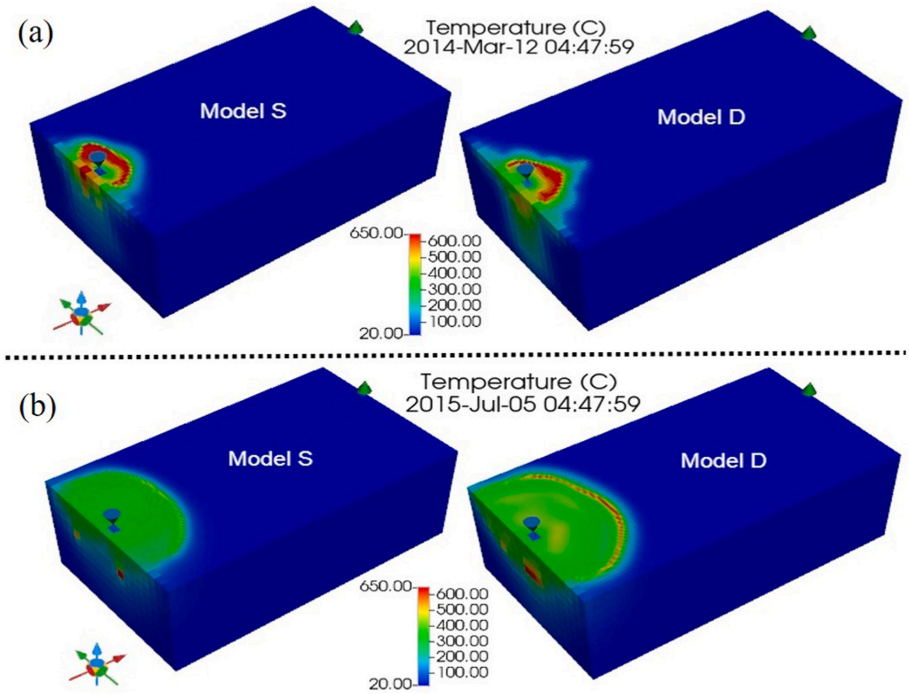

Fig. 17. 3D simulated temperature profile by Model S and Model D in (a) March 2014 and (b) July 2015.

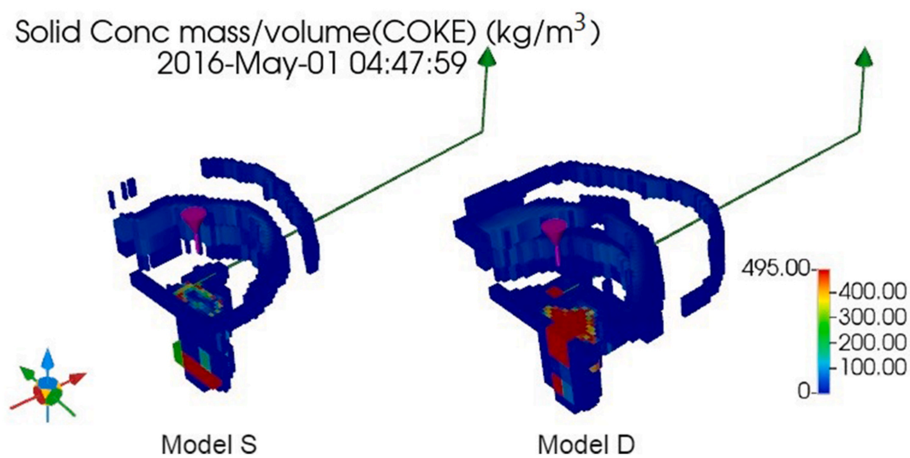

Fig. 18. Simulated 3D structure of the coke zone in Model S and Model D in May 2016.

study. Xia et al. (2003) reported that coke acts as a gas seal in the horizontal producer, preventing air channelling through (from behind the combustion front). Therefore, there was no oxygen production in their study. Jinzhong et al. (2012) experimentally showed that the sealing ability of the coke zone and the operating parameters are closely related. It was reported that after the combustion front propagates beyond the toe position of HP, the oxygen will break through the coke zone and flow directly into the HP if the injection parameters are improper (e.g., too high air injection rates and/or injection pressure). The coke layer served as a gas seal ahead of the combustion front in the present study. However, coke did not prevent O_2 breakthrough into the HP when the combustion front was beyond the toe section of the HP. Hence, the relationship between coke generation and oxygen concentration around the horizontal producer was investigated in models S and D. The same area around the HP, in both models S and D, was selected for this examination. Fig. 19 presents this analysis for the third perforation from the toe side of the HP, as well as air injection rates for both models.

Model S predicted no coke deposition around the targeted area for the whole 30 months of simulated period. This indicates that insufficient heavy oil thermal cracking took place at this region during the THAI process, which will be investigated later in detail. The primary oxygen breakthrough (although below 3%) into the region was detected in late-Sep 2014 (start of uninterrupted air injection). Simulated results by Model S indicate that the O_2 profile within the region experienced some fluctuations purely because of the variations in air injection rates until early-Feb 2015. The oxygen concentration was close to zero between early-Feb 2015 and mid-Apr 2015. This is most likely due to lower air injection rates during this period (30,000 m^3/day) and higher O_2 concentration around the second perforation from the toe side of the HP (shown in Fig. 14). The variation in air injection was within 10,000 m^3/day from the mid-Apr to May 2016. Despite minor changes to injected air amounts in Model S, the oxygen profile rapidly amplified (up to around 9%) until May 2016 (end of simulation). This is due to the propagation of the combustion front and connection of the HP with a combusted zone that is 100% saturated with injected air.

The simulated results for Model D (shown in Fig. 19) demonstrated

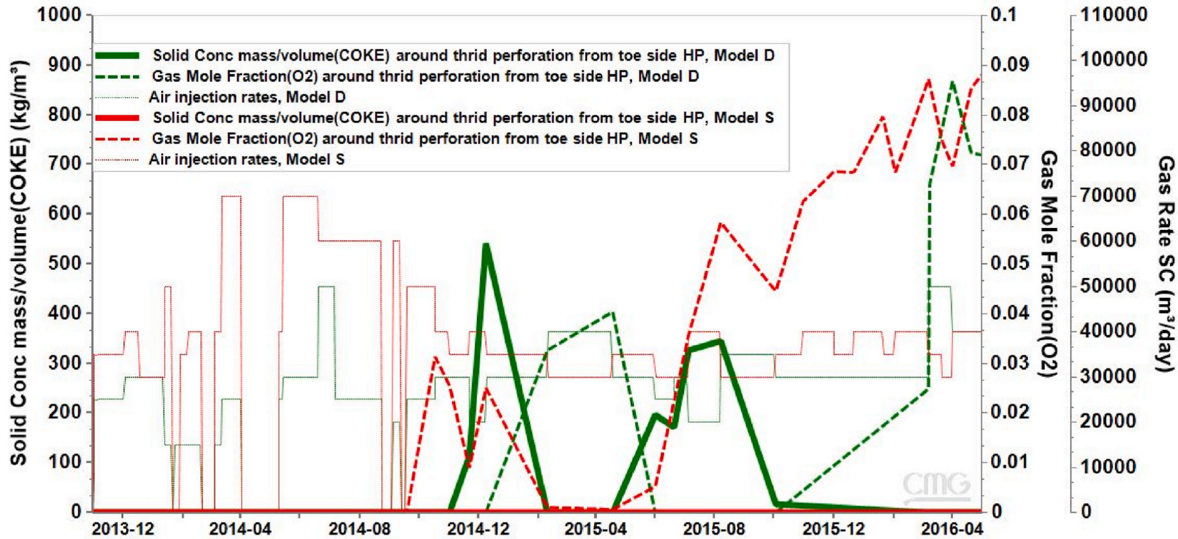

Fig. 19. Predicted coke concentration and oxygen profile around the third perforation from the toe side of HP in Model S and Model D. Notes: *SC stands for standard condition.

coke deposition from early-Nov 2014, with concentrations as high as around 500 kg/m^3 in Dec 2014. The oxygen breakthrough into the area (around the third perforation of the HP) began mid-Dec 2014 (with a sharp rate). Interestingly, this event coincided with a sharp decrease in coke concentration (as low as zero in early-Feb 2015) in the region. Coke concentration remained zero until late-Apr 2015, while the O_2 concentration in the gas phase increased up to 4%. It must be noted that air injection rates rose from 20,000 to 40,000 m^3/day between early-Dec 2014 and mid-Apr 2015, which contributed to oxygen breakthrough into the area. The second phase of coke deposition started in mid-April 2015 followed by a reduction in O_2 concentration in the area. It can be seen that the secondary coke build-up (up to 340 kg/m^3) happened immediately after a reduction in air injection rates from 40,000 to 20,000 m^3/day between mid-Apr 2015 and early-Aug 2015 in Model D. This emphasises the importance of air injection rates in providing the required heat for thermal cracking reactions in the reservoir. An increase in injected air rates, from 20,000 to 35,000 m^3/day, caused a drastic decrease in the deposited coke (as low as 15 kg/m^3 in early-Oct 2015) in the region. This was the point when the secondary oxygen breakthrough began. Another decline in air injection rates (even though it was minor) in early-Oct 2015, reduced the rate at which coke deposition was declining. During the next 5 months some coke deposition existed in the area, but this was below 15 kg/m^3. This kept oxygen concentration below 2.5% until early-Mar 2016. The sharp increase in O_2 profile that took place until the end of the simulated period is mainly related to the following three factors; a. no coke was present in the area, b. air injection rates increased to 50,000 m^3/day, and c. the area was in contact with 100% gas saturated combusted zone.

The above findings from models S and D in the present work clearly indicate that a lack of coke deposition around the exposed section of the HP leads to the development of high oxygen concentrations in the HP. Insufficient thermal cracking of crude oil is the main contributor to the low coke laydown. Thermal cracking of heavy oil was closely related to injected air rates. Model S had poor in-situ combustion performance at the toe section of HP leading to the absence of coke deposition. This was due to the extra air ingress from the KA5 injector well towards the KP2 producer well in Model S. Better thermal cracking took place around the toe section of the HP in Model D generating (even though partially) a coke seal around the exposed section of the HP. Consequently, serious oxygen breakthrough into the region was delayed in Model D compared to Model S. This means for existing THAI projects, such as the Kerrobert project, the selection of air injection must be made considering air flowing from neighbouring injector wells (it can be done by pausing air injection for a short period and recording the produced gas from the corresponding producer well).

5.4. Steam zone

The steam zone, that is generated during the THAI process, and its relationship with extra air flowing from KA5 are investigated in this section. Greaves et al. (2013) numerically studied the THAI process at field-scale, in which a steam zone was formed as the combustion front developed and propagated through the oil layer. They reported that steam was generated by evaporation of reservoir water and as a product of the combustion reactions. It was found that the steam zone was responsible for transporting the heat created by combustion reactions to the heavy oil. Three-dimensional studies of ISC by Greaves and Al-Honi (2000) showed that the thermal sweep efficiency is largely governed by the steam-gas front generated ahead of the combustion front, developing over the entire combustion period during ISC. They used a sand pack that had an initial water saturation of approximately 30% for their experiments. Both above studies did not consider bottom water for the reservoir. Therefore, it is important to study the generated steam zone during a THAI process in the presence of bottom water. The initial water saturation in the pay zone used for the present study is 26%. A transition zone (with 45% initial water saturation) and a bottom water zone (with 100% initial water saturation) are considered for the reservoir in this work.

Fig. 20 a and b show the steam profile at the horizontal midplane above the HP for models S and D, respectively, in Oct 2015. It is evident that the steam zone was larger in Model D compared to Model S. The expansion of the steam zone in models S and D (predicted in Apr, 2016) are shown in Fig. 20 c and d. A similar trend to that in Oct 2015 was observed for the formation of the steam zone in Apr (2016) (shown in Fig. 20 c and d). Poor ISC in Model S followed in a smaller steam zone, compared to Model D. It is fair to assume that the narrow steam zone was mainly generated from evaporation of reservoir water in Model S. Water vaporisation did not occur due to heat generation by ISC in model S. Reservoir water (in the pay zone) evaporated because of having contact with hot mobilised oil that was draining (downward) into the HP. On the other hand, a relatively large and constant extension of the steam zone took place during the THAI process simulated by Model D. This is more attributed to good ISC performance than evaporation of reservoir water in Model D. Subsequently, a higher amount of heat was transferred to

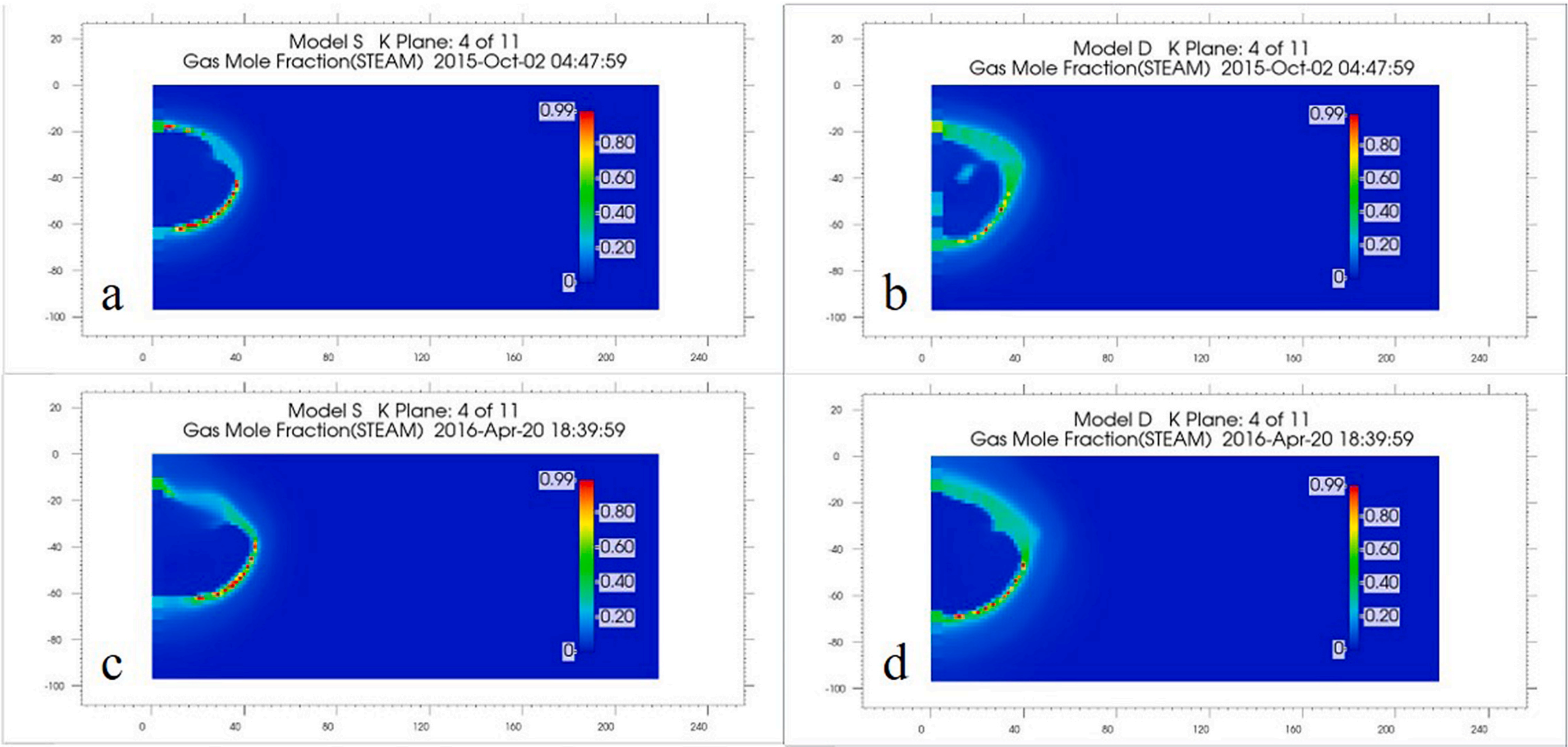

Fig. 20. Predicted steam profile by model S and D during THAI process.

the cold oil zone which led to greater thermal heavy oil mobilisation. The displacement of hot mobilised oil will be examined in Section 5.5 in detail. It must be noted that the predicted temperature profile for the bottom water zone, for both models, was below the boiling temperature for water at reservoir pressure during the simulated period. This means that the bottom water did not contribute to “extra” steam generation during the ISC process in Model S and Model D. Temperatures as high as 80 °C were predicted at a small portion of the BW area below the inlet zone. However, the temperature of the vast majority of the BW zone was unchanged during the simulated period for both models. This implies that the bottom water does not act as a heat sink during the ISC operation in both models, despite the consequences of the variation in air injection rates.

The THAI’s in-situ combustion nature has advantages over SAGD (in which surface-generated steam is injected into the reservoir). Successful ISC can dramatically lower the need for water and natural gas, with potentially smaller surface footprint, in comparison with steam injection (Kovscek et al., 2013). The predicted steam profiles in this present study once again indicates the importance of air injection rates for a successful THAI project. Effective steam generation is key for in-situ heat transfer, and this can be achieved by injecting the right amount of air that would maintain ISC propagation throughout THAI operation, even with the presence of bottom water in the reservoir.

5.5. Mobile oil zone (MOZ)

Fig. 21 shows the predicted oil saturation profile in the vertical midplane of models S and D. The region behind the combustion front (combusted zone with 100% gas saturation) was excluded from the vertical midplanes in Fig. 21. It is evident that, as the combustion front expanded in size and moved further away from the inlet zone, heat (coming either by conduction via the combustion front or by convection via steam) was transferred into the downstream oil region. This caused the MOZ to develop for the whole duration of the ISC. The MOZ contains two regions, namely region 1, which consists of the thermally cracked oil as well as lighter vaporized fractions, and region 2, which consists of the banked oil zone (BOZ) where the oil saturation is close to 100% (Greaves, et al., 2012 b). Earlier water production, from the inlet zone of the reservoir (where initially $S_o = 0.74$), formed the BOZ ($S_o = 1$) during the initialisation period of ISC. This is due to higher mobility of water compared to oil. The oil flux vectors, shown in Fig. 21, represent the direction in which the mobilised oil flow into the horizontal producer within the reservoir.

As discussed earlier, the extra air ingress from the neighbouring air injector well impacted the ISC efficiency in a negative way in Model S. Therefore, the BOZ, that was developed and extended by steam, is the major source for the MOZ in Model S. Good oil production rates were predicted for Model S (a peak of approximately 30 m^3/day shown in Fig. 6) in late-Sep 2014. This was caused by (1) reinjection of a high volume of air into the reservoir (after a short break in mid-Sep 2014) and (2) oil flow into the toe of the HP from the previously established BOZ in model S (displayed by the forward directed horizontal vector in Fig. 21 a). Also, the gravity drainage of mobilised oil into the exposed section of the HP closer to the heel (shown by vertically downwards vectors in

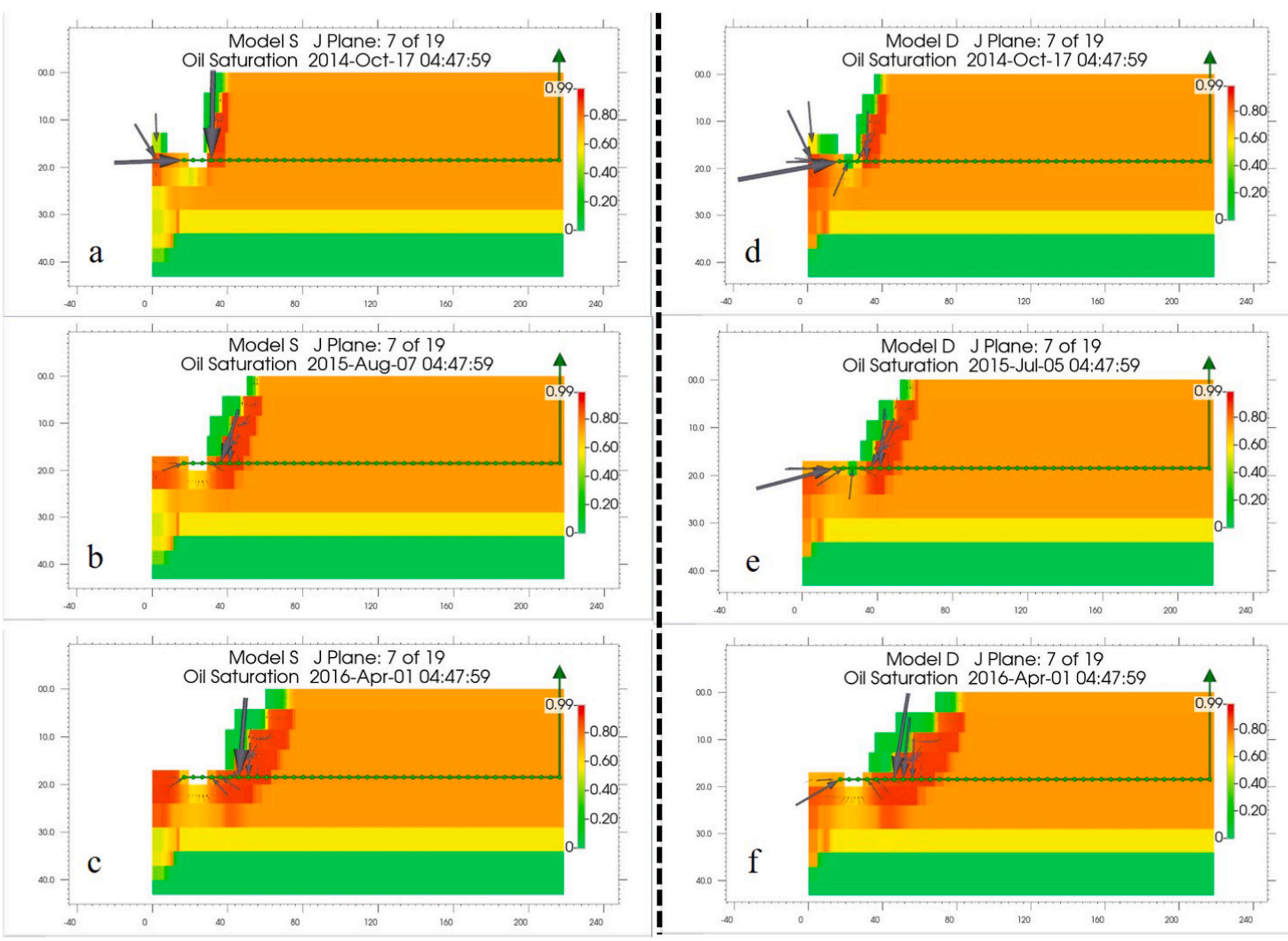

Fig. 21. Predicted oil saturation profile by model S and D during uninterrupted air injection period.

Fig. 21 a), contributed to the prediction of peak oil rate. Fig. 21 d exhibits a similar pattern of oil displacement as simulated for Model S at the same time. However, a greater volume of oil flowed into the toe section (bigger oil flux vector shown in Fig. 21 d) which resulted in a peak of 45 m^3/day in oil production. This was related to the larger BOZ (higher oil saturation) around/below the toe section of HP in Model D. Looking at Fig. 21 b and e, the BOZ ahead of the combustion front in model S was the same as Model D in size. The predicted oil production by model S was mainly limited to gravity drainage in Aug 2015. Whereas, a considerable amount of oil was produced from the toe section of HP in Model D during the same period. Another noticeable event was that the second and third perforation of the HP from the toe side in Model S were fully saturated by gas in Aug 2015. Mobilised oil was produced from the same location (flowed from beneath the HP), at the same time, in Model D. The second and third perforations of the HP from the toe side in Model D became 100% saturated by gas in Model D in late 2015. Although a lower amount of oil was produced from below the HP in Model D (almost equal to Model S), higher volumes of mobilised oil drained into the HP from the upper part of the reservoir in Apr (2016) (demonstrated in Fig. 21 c and f). This was due to the significant increase in the size of BOZ ahead of the combustion front in Model D compared to its size in Aug 2015. Also, the BOZ ahead of the combustion front is larger in Model D compared to Model S in Apr (2016), displaying better combustion front advancement along the HP in Model D. The cold oil zone (COZ) was undisturbed during the THAI process in this study as no oil displacement was detected by both models in the COZ. The substantial difference in predicted daily oil production rates by models S and D (shown in Fig. 16), from Aug 2015 until the end of simulated period, reflects the abovementioned events.

Additionally, the oil saturation profile in Fig. 21 illustrates that some of the mobilised oil sank into the transition and bottom water zones in both models throughout the THAI process. Hence, a considerable amount of oil was left behind (trapped) in the deeper portion of the reservoir. This was a common issue for models S and D. This means that variation in air injection rates, employing the same THAI well arrangement, could not prevent mobilised oil sinking to the bottom water. A potential solution, to capture the maximum possible mobilised oil, is to move the HP closer to the transition zone. Model S was used to investigate the effect of HP location. It was also examined whether poor oxygen utilisation in Model S can be improved by adjusting the HP position. Two models were constructed (based on operating parameters of Model S) with adjusted HP positions, referred to as Model HP6 and Model HP7. It must be noted that the horizontal producer was placed 5 and 10 m closer to transition zone in models HP6 and HP7 respectively. Fig. 22 exhibits simulated results by models HP6 and HP7. It is evident that mobilised oil sank into bottom water zone in both model HP6 and HP7, no matter how close to transition zone the HP was (displayed in Fig. 22 a and b). Therefore, a variation in HP location could not prevent oil sinking into deeper layers in the reservoir.

Fig. 22 c shows that all three models predicted a similar initial oil production profile. However, from May 2014, a deviation in simulated cumulative oil production profiles occurred. Model HP6 predicted 28% higher cumulative oil production compared to Model S. The oxygen utilisation was improved by 5% in model HP6 in comparison with Model S. Model HP7, with the HP placed just above the transition zone, predicted better oil recovery performance amongst the three models. The oxygen utilisation was improved to 86% in model HP7 resulting in 73% higher cumulative oil production compared to Model S. Overall, the simulation results demonstrate that the closer the HP was located to the transition zone, the higher the oil recovery that was achieved. In other words, the K2 THAI pilot well pair could have produced more oil by placing the KP2 well at a level closer to transition zone, including the effect of extra air ingress from KA5.

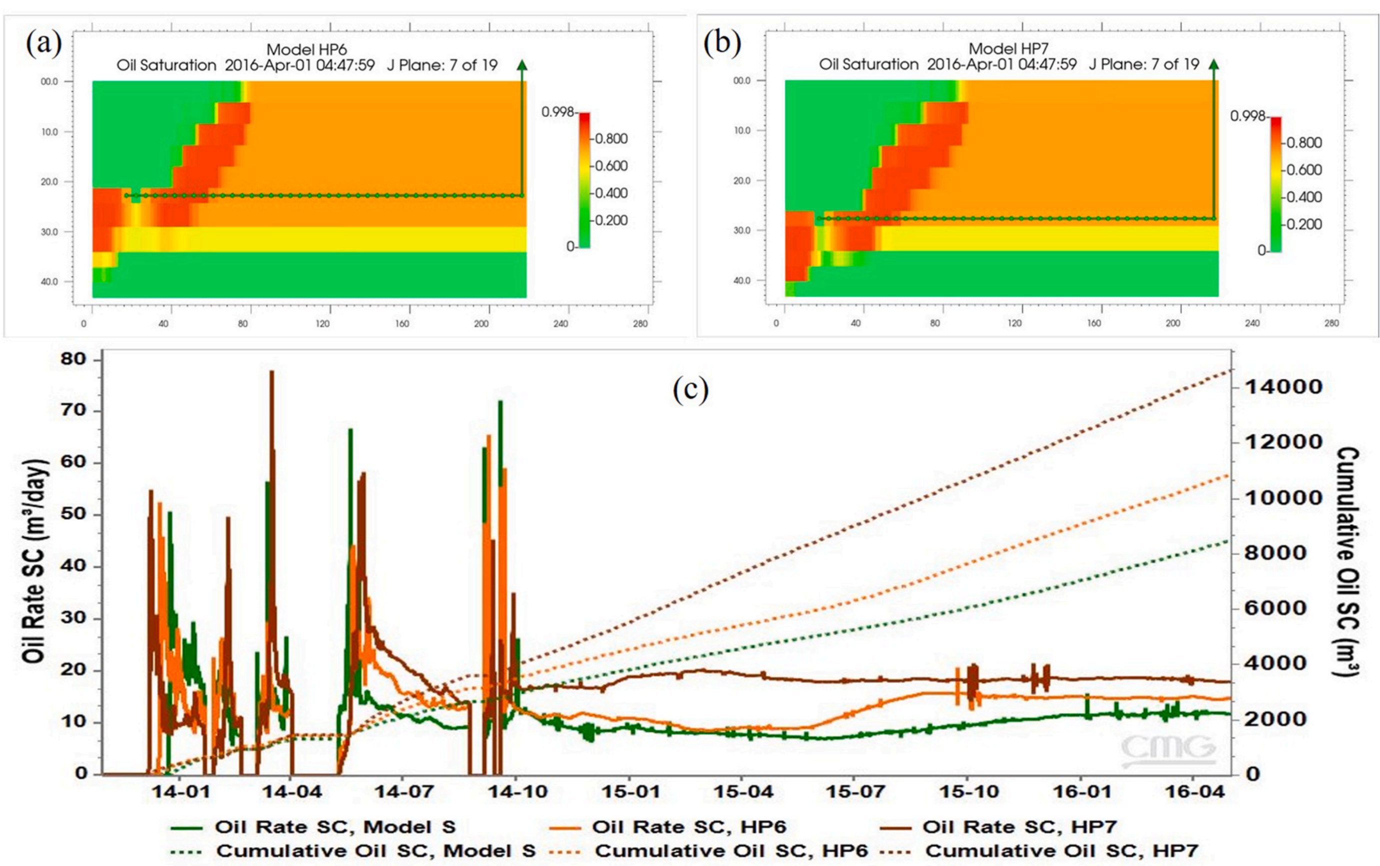

Fig. 22. Predicted oil saturation profile (a and b) and oil production profile by model S with varied HP location (c).

6. Conclusion

The field data analysis in this work indicates that the K2 pilot, one of the best performing THAI well pairs in the Kerrobert project, suffered interference from a neighbouring K5 semi-commercial THAI well pair. The air injected through KA5 flowed in a direction opposite to that intended, namely towards the K2 pilot. This caused a significant imbalance between injected air and produced gas for KA2 and KP2, respectively. Previously developed field-scale THAI models lacked a. consideration of a bottom water zone in the reservoir and b. validation against the actual field data. In addition, previous numerical studies reported a proportional relationship between air injection rates and oil production rates in the THAI process. In present work, a new field-scale THAI model with relatively thick bottom water layer was developed and validated against the Kerrobert field data. The simulation was used to probe whether the air injection rates impact the overall performance of the THAI process in the presence of bottom water. It was found that excessive air injection reduced oxygen utilisation resulting in a poor ISC efficiency with combustion time. This means more air injection does not necessarily promote oil production in the THAI process in a bottom water situation. The O_2 utilisation was improved from 74 to 90% by restricting air injection to only that into KA2 alone itself. This means the interference from the KA5 has negatively impacted the overall performance of the K2 pilot. Various developed zones throughout the combustion front propagation were investigated in this study. It was numerically shown that extra air ingress from KA5 has had a negative impact on the combustion temperature profile. Similar to previous studies, the coke zone served as a gas seal preventing oxygen channelling ahead of combustion front in the new model. An inversely proportional relationship was detected between coke concentration and oxygen profile around the horizontal producer (HP) in this work. It was also found that the size of the steam zone varies with changes in air injection rates. The MOZ analysis demonstrates that a large BOZ was developed below the HP during THAI operation. Relocation of the horizontal producer was proposed as a potential strategy to capture as much mobilised oil as possible. The oxygen utilisation was improved by 13%, resulting in 73% higher cumulative oil production in comparison with the history matched model.

Therefore, the following suggestions can be made for optimisation purposes: a. for forthcoming projects, THAI well pairs must be drilled at a sufficient distance to prevent unwanted interferences from each other, unless the operation is based on intended interaction between air injector wells (e.g., staggered line drive (SLD) THAI well arrangement), b. for existing THAI projects such as Kerrobert, the selection of air injection must be made considering air flowing from neighbouring injector wells (it can be done by pausing air injection for a short period and recording the produced gas from the corresponding producer well), and c. HP locations closer to the transition zone could be considered in order to produce from the large BOZ developed below the HP, and enhance oil recovery.

Credit author statement

Hossein Anbari: Conceptualization, Methodology, Investigation, Writing – original draft, Visualization. **John P Robinson**: Supervision, Validation; **Malcolm Greaves**: Supervision, Validation.; **Sean P Rigby**: Supervision, Recourses, Validation, Writing – review & editing.

Declaration of competing interest

The authors declare that they have no known competing financial interests or personal relationships that could have appeared to influence the work reported in this paper.

Data availability

The source of history matching data from the Kerrobert THAI project has been shared in references section (available at www.petrobank.ca).

Acknowledgement

This work was supported by the Natural Environment Research Council (NERC) Centre for Doctoral Training (CDT) in Oil & Gas [grant number NE/M00578X/1]. Sean P Rigby, John Robinson, and Hossein Anbari thank the University of Nottingham for the award of a PhD studentship. We would like to thank Dr. Alex Turta for providing us with the Comprehensive Assessment of the THAI report. We would also like to thank Mr. Konstantin Starkov (former operating manager of Petrobank Energy Ltd in the Kerrobert THAI pilot project) for providing us with the production history of the K2 THAI pilot and his supportive communications during this study. We thank CMG for support with the STARS software.

References

Adam, M., et al., 2020. In-situ microwave-assisted catalytic upgrading of heavy oil: experimental validation and effect of catalyst pore structure on activity. Chem. Eng. J. 413, 127420.
Ado, M.R., 2019. Simulation study on the effect of reservoir bottom water on the performance of the THAI in-situ combustion technology for heavy oil/tar sand upgrading and recovery. SN Appl. Sci. 2–29.
Ado, M.R., 2020 a. A detailed approach to up-scaling of the Toe-to-Heel Air Injection (THAI) In-Situ Combustion enhanced heavy oil recovery process. J. Petrol. Sci. Eng. 187, 106740.
Ado, M.R., 2020. Predictive capability of field scale kinetics for simulating toe-to-heel air injection heavy oil and bitumen upgrading and production technology. J. Petrol. Sci. Eng. 187 (106843), 106843.
Ado, M.R., Greaves, M., Rigby, S.P., 2017. Dynamic simulation of the toe-to-heel air injection heavy oil recovery process. Energy Fuel. 31 (2), 1276–1284.
Ado, M.R., Greaves, M., Rigby, S.P., 2022. Numerical simulation investigations of the applicability of THAI in situ combustion process in heavy oil reservoirs underlain by bottom water. Petroleum Research.
Araujo, E.A., et al., 2016. Analysis of oil production by applying in situ combustion. Petrol. Sci. Technol. 34 (1), 50–55.
Ayasse, C., et al., 2005. First Field Pilot of the Thai Process. Petroleum Society/Canadian Institute of Mining, Metallurgy & Petroleum, Calgary, Canada.
Baker, R.O., Chugh, S., Mcburney, C., Mckishnie, R., 2006. History matching standards; quality control and risk analysis for simulation. In: Canadian International Petroleum Conference. Calgary, Canada.
Coates, R., Zhao, L.L., 2001. Numerical evaluation of THAI process. In: Canadian International Petroleum Conference. Calgary, Canada.
Donnelly, J.K., Pendergast, D.K., 1999. Nuclear Energy in Industry: Application to Oil Production. Canada, Montreal (s.n).
Greaves, M., Dong, L.L., Rigby, S.P., 2012a. Determination of limits to production in THAI. Calgary. In: SPE Heavy Oil Conference Canada. Canada.
Greaves, M., Al-Honi, M., 2000. Three-dimensional studies of in situ combustion-horizontal wells process with reservoir heterogenties. J. Can. Petrol. Technol. 39 (10), 25–32.
Greaves, M., Al-Shamali, O., 1996. In situ combustion (ISC) process using horizontal wells. J. Can. Petrol. Technol. 35, 49–55.
Greaves, M., Dong, L.L., Rigby, S.P., 2012 b. Validation of toe-to-heel air injection bitumen recovery using 3D combustion-cell results. In: SPE EUROPEC/EAGE Annual Conference and Exhibition. Vienna, Austria.
Greaves, M., Dong, L.L., Rigby, S.P., 2013. Toe-to-Heel air injection- effect of oil layer thickness. In: 17th Eauropean Symposium on Improved Oil Recovery. St. Petersburg, Russia.
Greaves, M., et al., 2001. THAI - new air injection technology for heavy oi recovery and in situ upgrading. J. Canadian Petrol. Technol. 40 (3), 38–47.
Hill, P., 2017. *Hydrocarbon Distribution In the Mannville Waseca Member, Edam Oil Field, West-Central Saskatchewan,* Regina, Canada: Saskatchewan Geological Survey, Saskatchewan Ministry of the Economy.
International Energy Agency, 2021 [Online] Available at: Energy Outlook 2021. Accessed 20 10 2021. https://www.iea.org/reports/world-energy-outlook-2021.
Jinzhong, L., et al., 2012. Progagation and control of fire front in the combustion assisted gravity drainage using horizontal wells. Sinece Direct 39 (6), 764–771.
Kovscek, A.R., Castanier, L.M., Gerritsen, M.G., 2013. Improved predictability of in-situ-combustion enhanced oil recovery. SPE Reservoir Eval. Eng. 16 (2), 172–182.
Nasr, T.N., Ayodele, O.R., 2005. Thermal Techniques for the Recovery of Heavy Oil and Bitumen. Society of Petroleum Engineers, Kuala Lumpur, Malaysia.
Petrobank Energy, Recources Ltd, 2021 [Online] Available at: Kerrobert THAI project production history. Accessed 06 05 2021. https://petrobank.ca/.
Petrobank Energy & Resources Ltd, 2012. Annual Report. Petrobank Energy & Recources Ltd, Calgary, Canada.

Shah, A., et al., 2010. A review of novel techniques for heavy oil and bitumen extraction and upgrading. Energy Environ. Sci. (3), 700–714.
Turta, A., 2021. Toe-to-Heel Air Injection (THAI) Process: Lessons from 14-Year Field Experience. A T EOR Consulting Inc, Calgary, Canada.
Turta, A., Greaves, M., Grabowski, J., 2018. Comprehensive assessment of toe-to-heel air injection (THAI) process. In: Guidelines for Development of Future Generations of In-Situ Combustion Processes. A CO-OPERATION BETWEEN A.T. EOR CONSULTING INC. SUILVEN OIL & GAS LTD AND PETRO MANAGEMENT GROUP (PMG), Calgary, Canada.
Turta, A., Greaves, M., Strakov, K., 2021 [Online] Available at: Adv. THAI Brochure. Accessed 10 10 2021. https://www.insitucombustion.ca/Advanced_THAI_Brochure.pdf.
Turta, A., kapadia, P., Gadelle, C., 2020. THAI process: determination of the quality of burning from gas composition taking into account the coke gasification and water-gas shift reactions. J. Petrol. Sci. Eng. 187, 106638.
Wei, W., Rezazadeh, A., Wang, J., Gates, I.D., 2021. An analysis of toe-to-heel air injection for heavy oil production using machine learing. J. Petrol. Sci. Eng. 197 (108109), 108109.
Wei, W., Wang, J., Afshordi, S., Gates, I.D., 2020. Detailed analysis of Toe-to-Heel Air Injection for heavy oil production. J. Petrol. Sci. Eng. 186 (106704), 106704.
Wikel, K., Kendall, R., 2012. 4D Study of Secondary Recovery Utilizing THAI from a Saskatchewan Heavy Oil Reservoir. Search and Discovery Article. Issue 90174.
Xia, T.X., Greaves, M., 2000. Upgrading Athabasca Tar Sand Using Toe-To-Heel Air Injection. Canada, Society of Petroleum Engineers, Calgary.
Xia, T.X., Greaves, M., 2006. In situ upgrading of athabasca tar sand bitumen using THAI. Chem. Eng. Res. Des. 84 (9), 856–864.
Xia, T.X., Greaves, M., Turta, A.T., Ayasse, C., 2003. THAI - A short-distanced displacement in situ combustion process for the recovery and upgrading of heavy oil. Chem. Eng. Res. Des. 81 (3), 295–304.